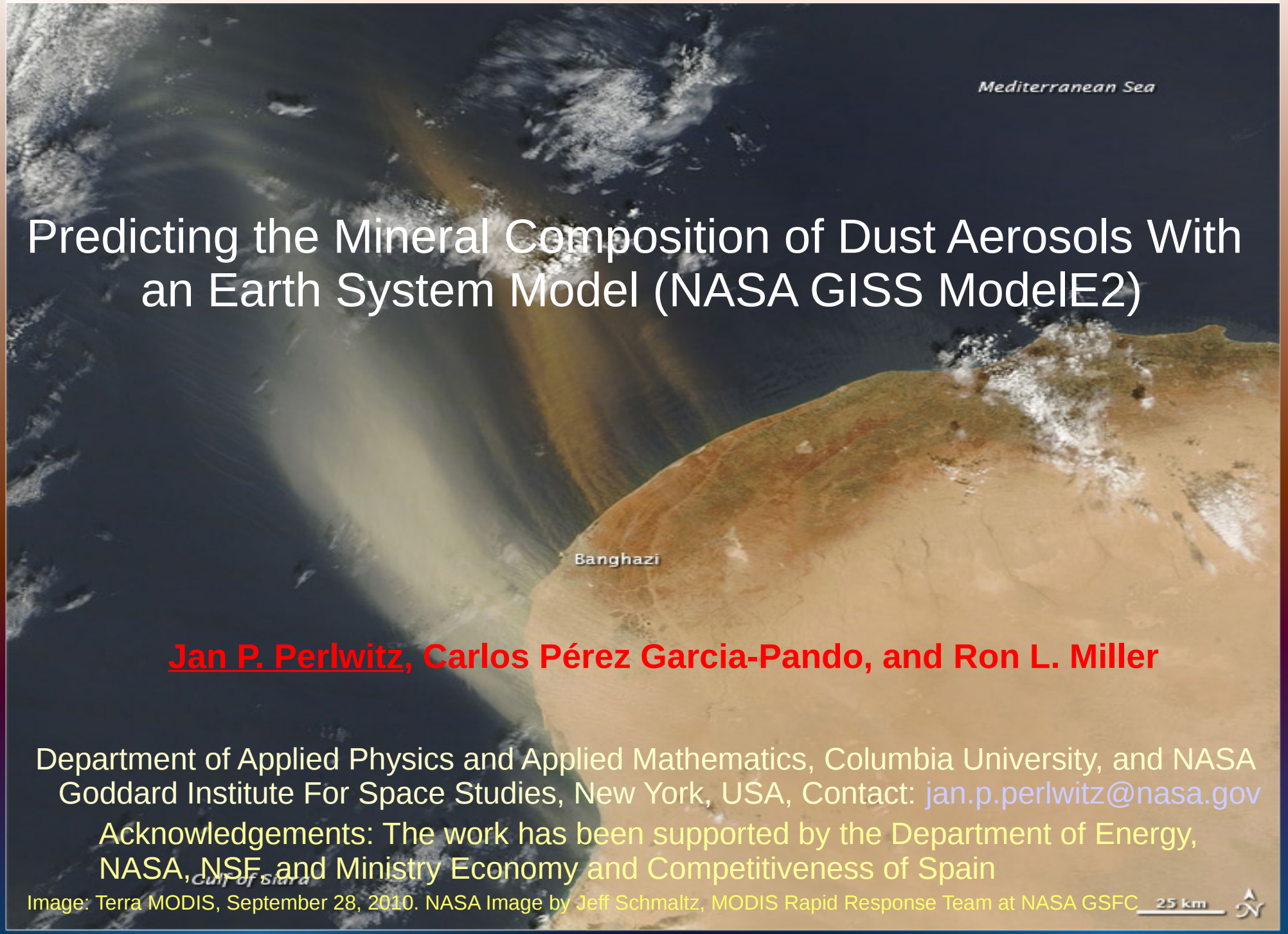

Predicting the Mineral Composition of Dust Aerosols With an Earth System Model (NASA GISS ModelE2)

Jan P. Perlwitz, Carlos Pérez Garcia-Pando, and Ron L. Miller

Department of Applied Physics and Applied Mathematics, Columbia University, and NASA Goddard Institute For Space Studies, New York, USA, Contact: jan.p.perlwitz@nasa.gov

Acknowledgements: The work has been supported by the Department of Energy, NASA, NSF, and Ministry Economy and Competitiveness of Spain

Image: Terra MODIS, September 28, 2010. NASA Image by Jeff Schmaltz, MODIS Rapid Response Team at NASA GSFC

Outline

1. Soil (mineral) dust aerosols in Earth's climate system
2. Globally uniform soil dust in ModelE
3. Predicting the mineral composition of dust aerosols in ModelE
4. Outlook to next steps and near future work

Soil Dust Aerosols in the Climate System

- Major aerosol in the atmosphere (global emission 1000-3000 Tg/a; total mass load in atmosphere approximately 20-35 Tg)
- High spatial and temporal variability
- Absorbs and reflects radiation => impact on radiation balance, warming or cooling effect depending on the single scattering albedo of the dust particles
- Carrier of nutrients like iron => Fertilization of phytoplankton => Carbon cycle
- Cloud condensation nuclei, ice nuclei
- Atmospheric chemistry (e.g., uptake of SO_2, H_2SO_4, HNO_3, N_2O_5, NO_3, NO_2, O_3, H_2O_2, OH, HO_2) => formation of coatings, like sulfates, nitrates, and/or effect on trace gas budgets

Dust Particles

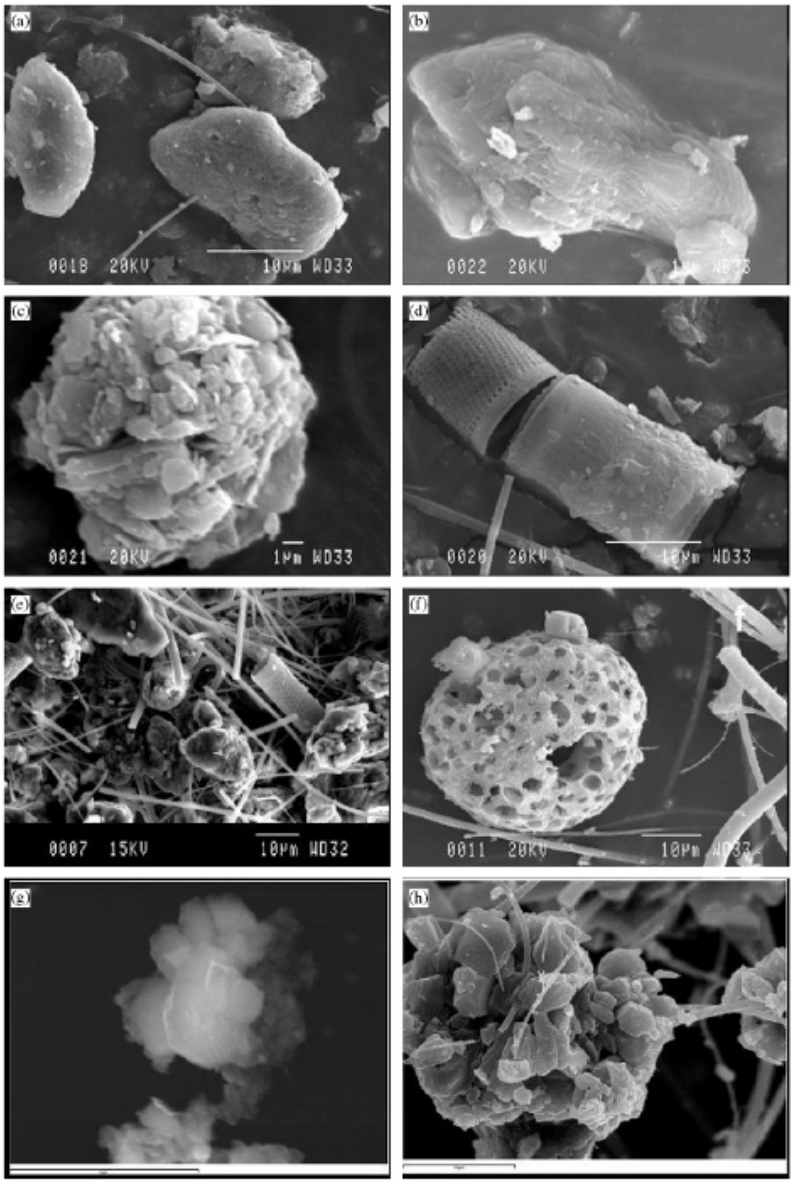

Fig. 5. SEM microphotographs of TSP collected the 29th July 2002 at IZO (a–d) and at SCO (e–h). IZO: (a) rounded quartz; (b) large (>10 µm) plate clay particles; (c) aggregates of micro-crystals of clay minerals; (d) silica skeletons of fresh water diatom from the *Melosira* genus, present in lakes or ponds from Northern Africa. SCO: (e) general aspect showing the presence of mineral dust, marine aerosol and *Melosira* genus diatoms, coated with sulphate; (f) spongy carbonaceous particles with sodium chloride crystals from marine aerosols; (g) K/Ca sulphate coating clay aggregates and (h) <5 µm Ca sulphate particles with crystalline habit.

(Alastuey et al., 2005)

Global Dust Sources

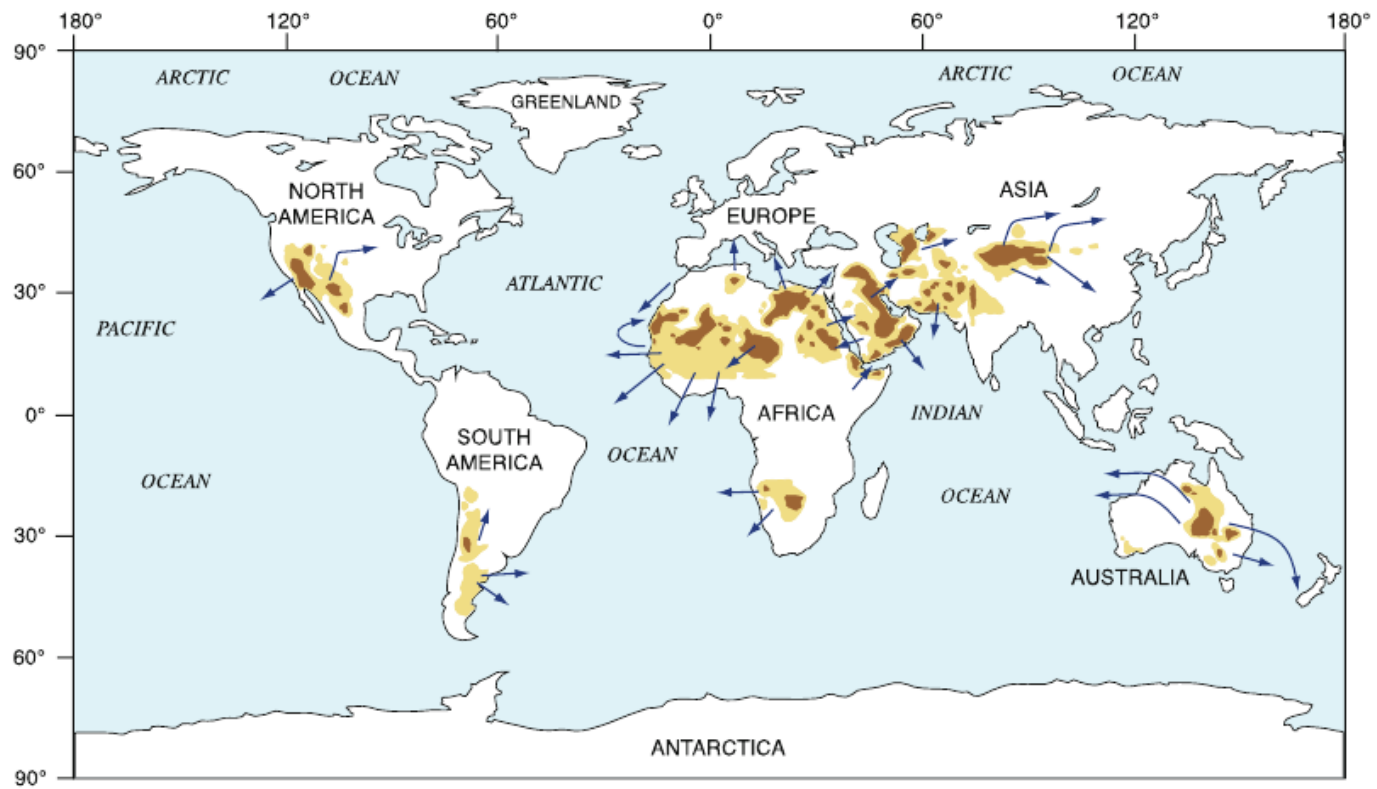

Fig. 3.2 Map of global dust sources, based on multiple years of satellite imagery, derived from frequency of occurrence (number of days) where the TOMS absorbing aerosol index (*AAI*) is greater than 0.7 (significant amounts of dust or smoke) or 1.0 (abundant dust or smoke). For comparison, nonabsorbing aerosols such as sulfate and sea salt yield negative AAI values; clouds yield values near zero; ultraviolet-absorbing aerosols such as dust and smoke yield positive values (Prospero et al. 2002). *Dark brown* is 21–31 days; *yellow* is 7–21 days (Redrawn from Fig. 4 of Prospero et al. 2002). *Blue arrows* indicate typical dust transport pathways, based on interpretation of MODIS imagery from Terra and Aqua satellites by the authors

(Muhs et al. 2014)

Global Dust Emission:
1000-3000 Tg/a
(Cakmur et al. 2006)

Northern Africa:
515 Tg/a
(Miller et al. 2004)
to 1087 Tg/a
(Tanaka and Chiba, 2006)

East Asia:
54 Tg/a (Luo et al., 2003)
to 460 Tg/year
(Laurent et al. 2006)

Arabian Peninsula:
43 Tg/a
(Miller et al., 2004)
to 496 Tg/a
(Ginoux et al., 2004)

Australia:
37 Tg/a
(Zender et al., 2003)
to 148 Tg/a
(Miller et al., 2004)

Mie Scattering and Absorption by Mineral Dust

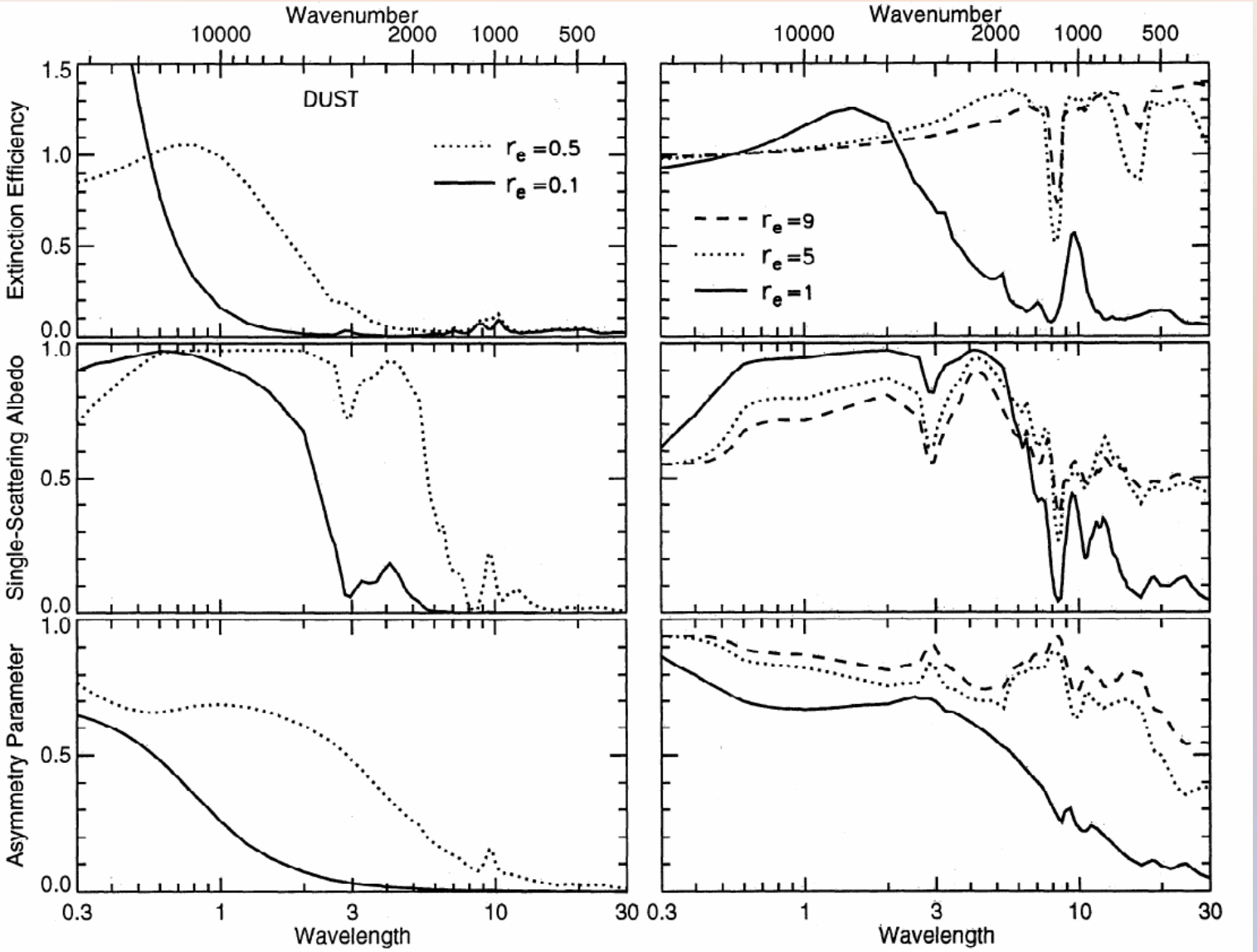

Figure 1. Mie scattering calculated radiative parameters for desert dust aerosol for eight particle sizes (effective radii, r_e, given in micrometers) in dependence on wavelength (in micrometers).

(Tegen and Lacis, JGR 1996)

Uncertainty in Radiative Properties of Mineral Dust

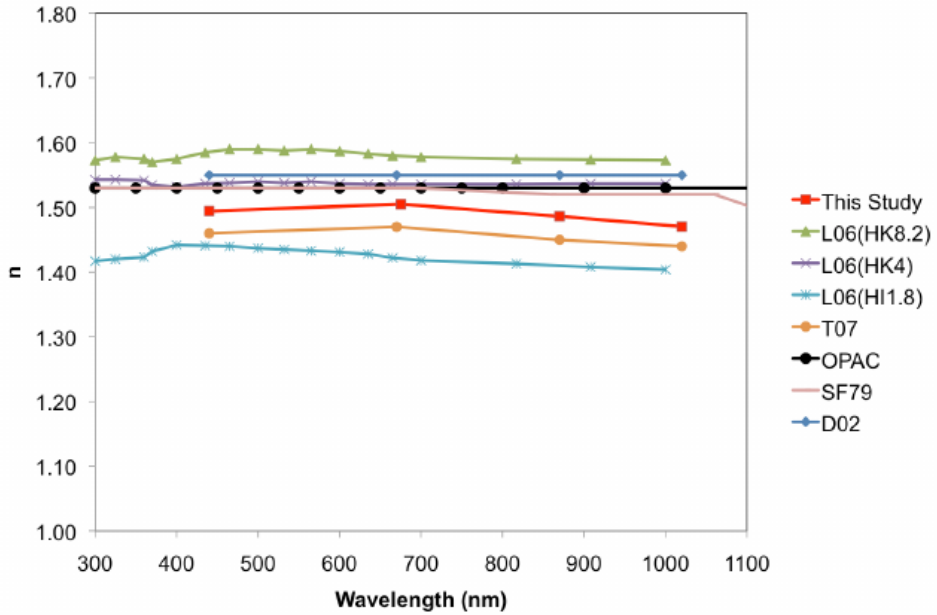

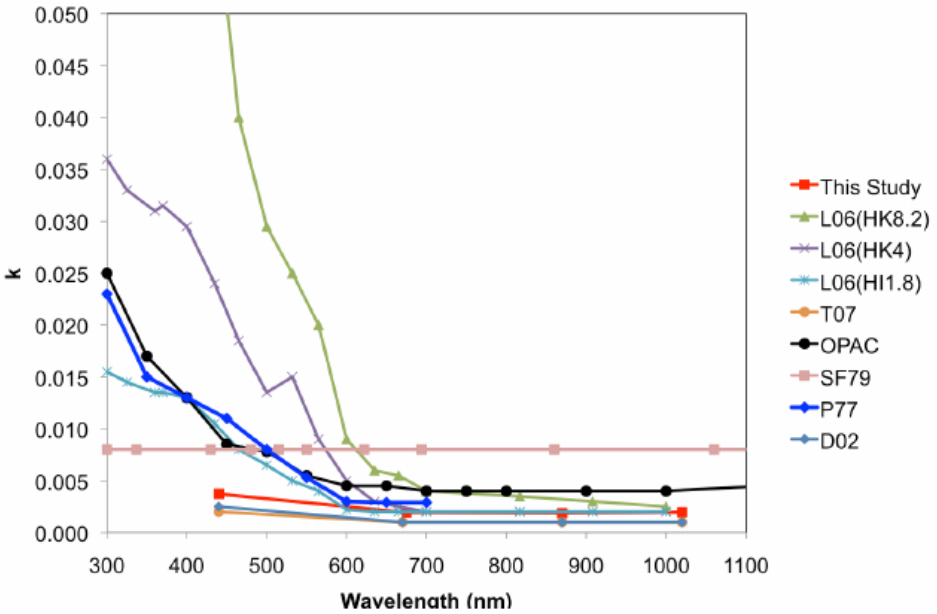

Fig. 5. Real and imaginary refractive index of the dust determined from AERONET (DU) from the current study. T07 is from Todd et al. (2007), OPAC is from Hess et al. (1998), SF79 is from Shettle and Fenn (1979), L06 is from Lafon et al. (2006), and D02 is the Bahrain site (most abosrobing site) in Dubovik et al. (2002). Different volume fractions (%) of iron oxide in the hematite-kaolinite (HK) and hematite-illite (HI) aggregates are shown in the parenthesis of L06.

(Kim et al., ACP 2011)

Radiative Forcing by Soil Dust

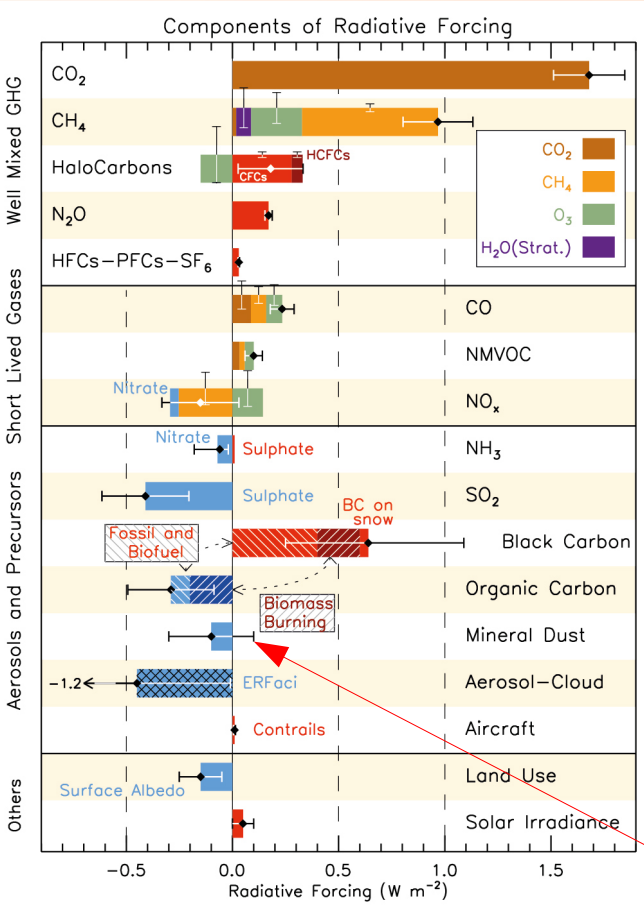

(IPCC, 2013)

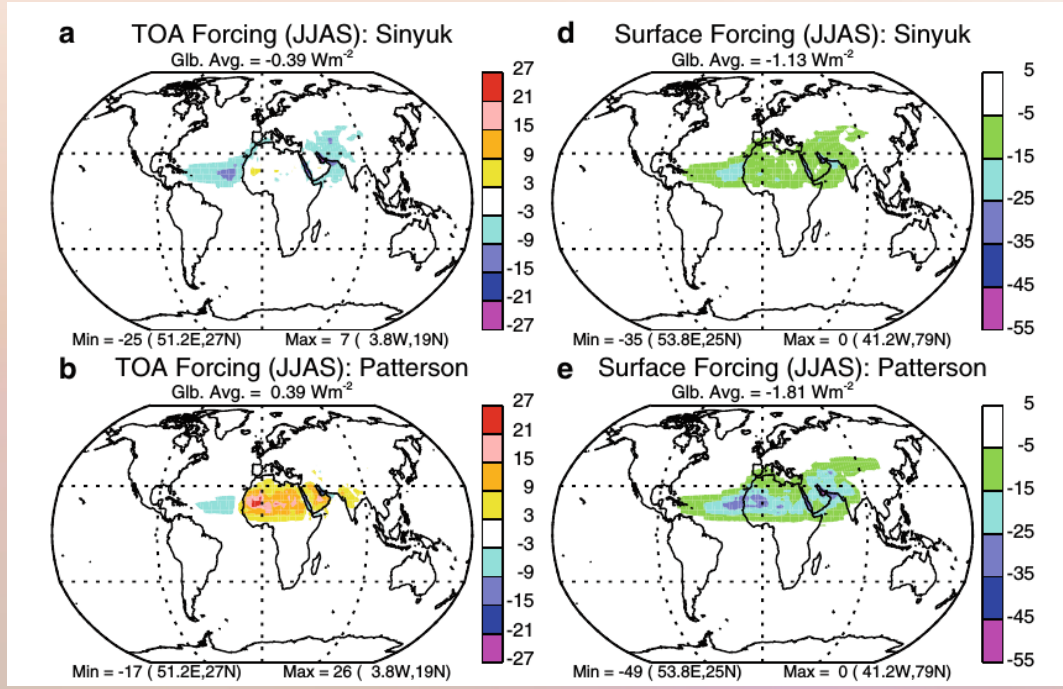

(Miller et al., 2014)

Mineral Dust

- Radiative forcing: Change in radiation flux before climate response
- Globally averaged top of atmosphere (TOA) radiative forcing by dust is relatively small, -0.4 to 0.4 W/m^2 (pre-industrial to present day, -0.3 to 0.1 W/m^2, for comparison TOA forcing by CO_2: ca. 1.9 W/m^2), globally averaged dust surface forcing always negative, larger in magnitude, < -1 W/m^2
- However, forcing by dust regionally much larger

Impact on Human Health

All *EHP* content is accessible to individuals with disabilities. A fully accessible (Section 508–compliant) HTML version of this article is available at http://dx.doi.org/10.1289/ehp.1306640.

Research

Soil Dust Aerosols and Wind as Predictors of Seasonal Meningitis Incidence in Niger

Carlos Pérez García-Pando,[1,2] Michelle C. Stanton,[3,4,*] Peter J. Diggle,[3,5] Sylwia Trzaska,[6] Ron L. Miller,[1,2] Jan P. Perlwitz,[1,2] José M. Baldasano,[7] Emilio Cuevas,[8] Pietro Ceccato,[6] Pascal Yaka,[9] and Madeleine C. Thomson[6,10]*

[1]NASA Goddard Institute for Space Studies, New York, New York, USA; [2]Department of Applied Physics and Applied Math, Columbia University, New York, New York, USA; [3]Lancaster Medical School, Lancaster University, Lancaster, United Kingdom; [4]Liverpool School of Tropical Medicine, Liverpool, United Kingdom; [5]Department of Epidemiology and Population Health, University of Liverpool, Liverpool, United Kingdom; [6]International Research Institute for Climate and Society, Palisades, New York, USA; [7]Barcelona Supercomputing Center–Centro Nacional de Supercomputación, Barcelona, Spain; [8]Izaña Atmospheric Research Center, Agencia Estatal de Meteorología, Tenerife, Spain; [9]Office of Civil Aviation and Meteorology General Direction, Ouagadougou, Burkina Faso; [10]Department of Environmental Health Sciences, Mailman School of Public Health, Columbia University, New York, New York, USA

*These authors contributed equally.

(Pérez García-Pando et al., EHP 2014)

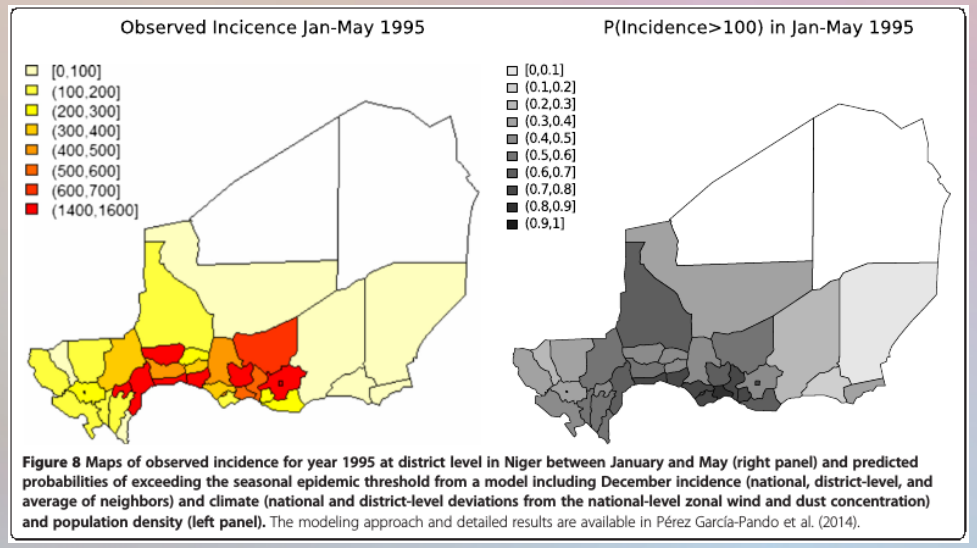

Figure 8 Maps of observed incidence for year 1995 at district level in Niger between January and May (right panel) and predicted probabilities of exceeding the seasonal epidemic threshold from a model including December incidence (national, district-level, and average of neighbors) and climate (national and district-level deviations from the national-level zonal wind and dust concentration) and population density (left panel). The modeling approach and detailed results are available in Pérez García-Pando et al. (2014).

(Pérez García-Pando et al., EP 2014)

Uniform Soil Dust in NASA-GISS ModelE2

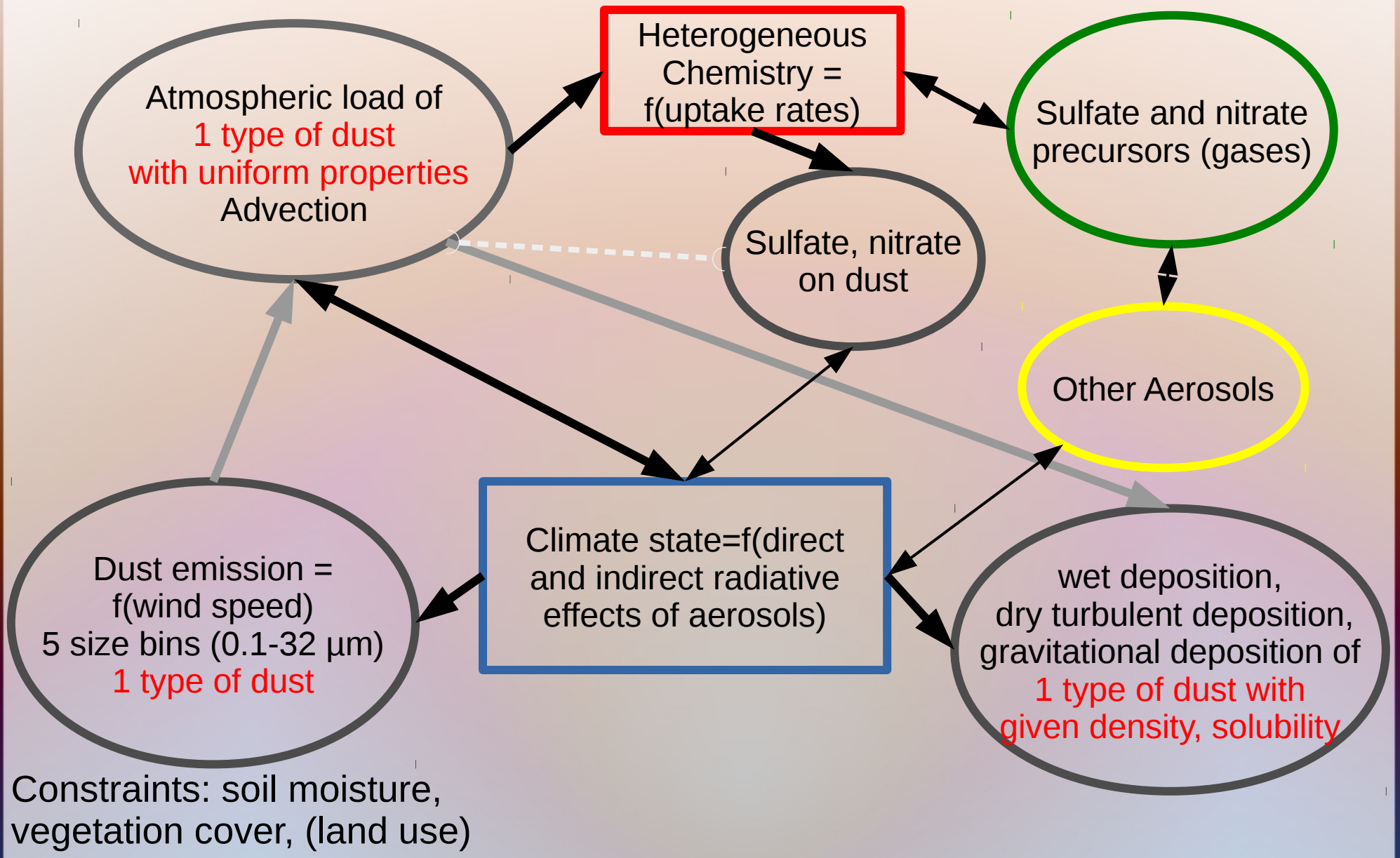

Constraints: soil moisture, vegetation cover, (land use)

Probability Scheme for Dust Emission

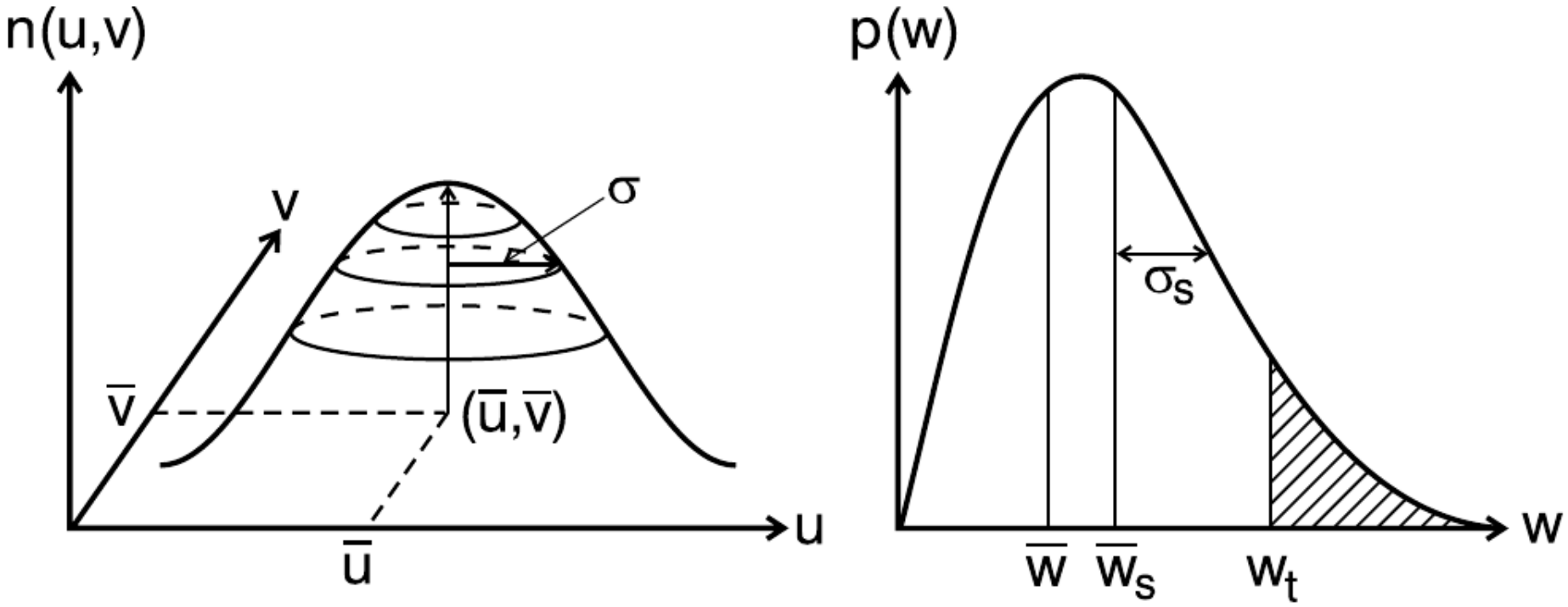

Figure 5. Probability functions representing the distribution of (left) wind velocity and (right) wind speed within the model grid box. Note that the mean wind speed $\overline{w}_s \equiv \int_0^\infty wp(w)dw$ is distinct from the speed of the mean wind $\overline{w} \equiv \sqrt{\overline{u}^2 + \overline{v}^2}$ that is explicitly calculated by the atmospheric general circulation model (AGCM). Similarly, the standard deviation of the wind speed, $\sigma_s \equiv \int_0^\infty (w - \overline{w}_s)^2 p(w)dw$, differs from σ, the standard deviation of each component of the wind velocity.

Cakmur et al., JGR (2004)

Globally Uniform Dust in ModelE (used up to CMIP5)

Optical Depth

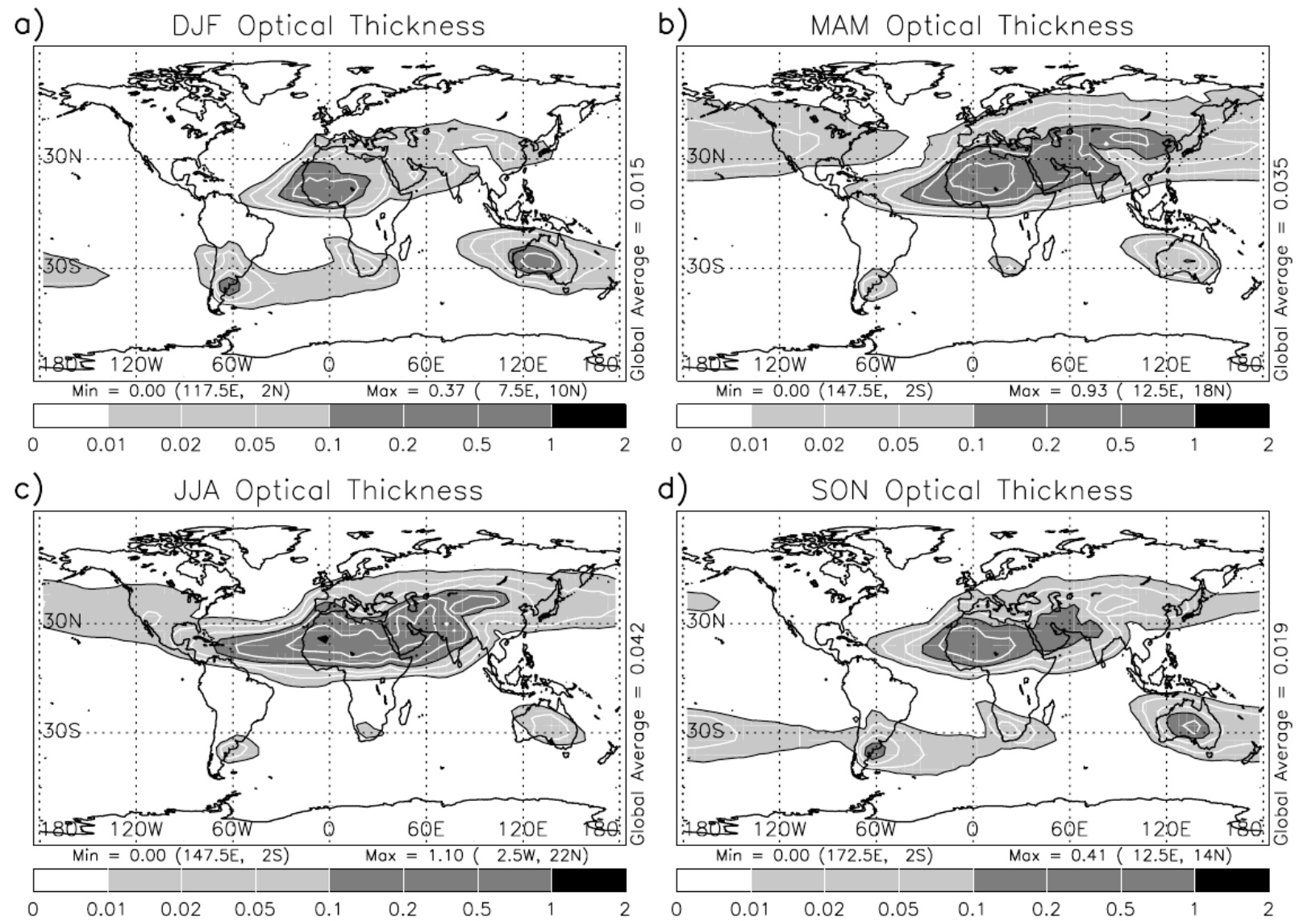

Figure 4. Clear-sky dust optical thickness for (a) DJF, (b) MAM, (c) JJA, and (d) SON.

(Miller et al., JGR 2006)

Globally Uniform Dust in ModelE (used up to CMIP5)

Single Scattering Albedo

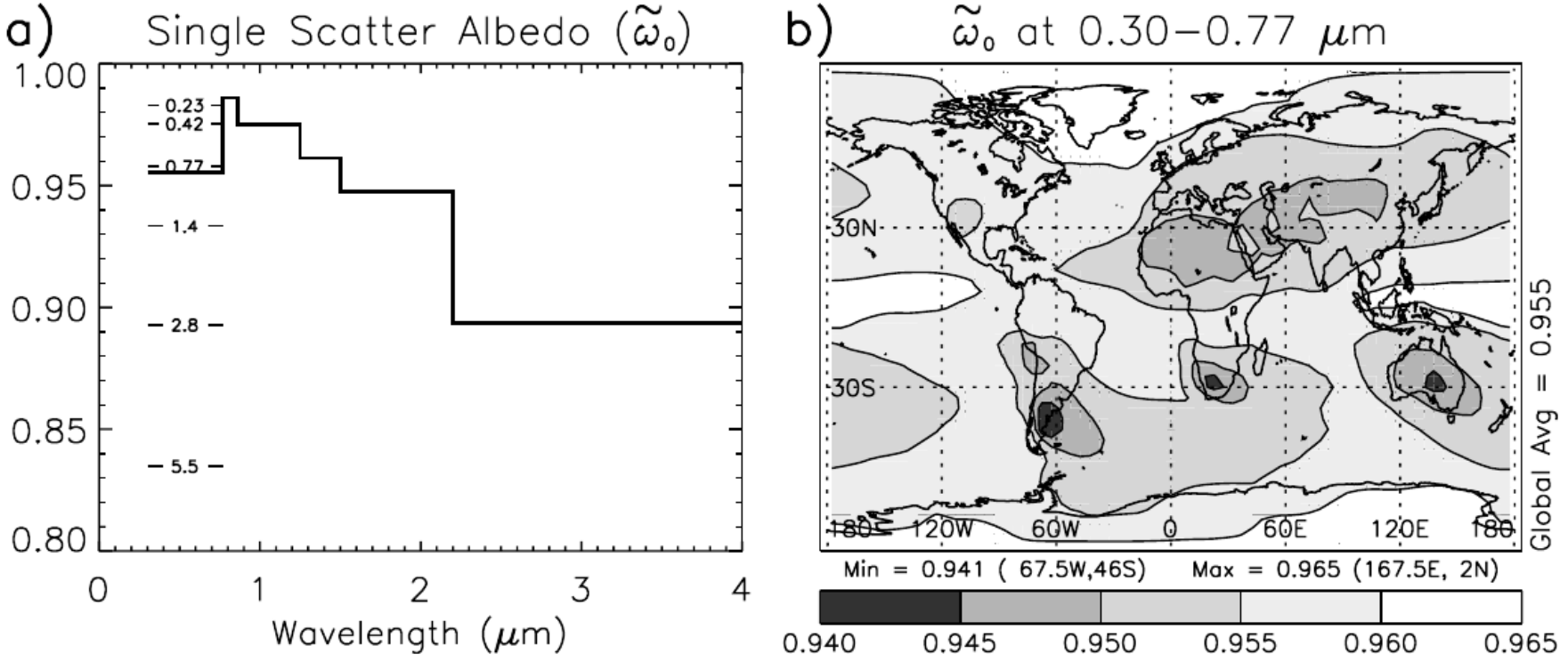

Figure 3. (a) Annual and global average of the bulk single scatter albedo ϖ_0, for the six spectral bands used in the calculation of solar radiative fluxes. The single scatter albedo is computed for each month as the ratio of the column scattering extinction and the column total extinction by dust. Also shown for the shortest solar band (0.30–0.77 μm) is the single scatter albedo for each individual particle size category, labeled by its effective radius. (b) Geographic distribution of the annual average bulk single scatter albedo at 0.3–0.77 μm.

(Miller et al., JGR 2008)

Why is the Mineral Composition of Soil Dust Important?

- Traditionally, global dust models have used globally uniform dust properties

Limitations for following reasons:

- Single scattering albedo (SSA) of dust particles depends on mineral composition, particularly on the mass fraction of hematite or goethite
- In turn, aerosol forcing and the response of clouds and atmospheric circulation to the forcing depend on the SSA
- Heterogenous chemistry (e.g., uptake rates) of dust particles depends on mineralogical and chemical composition
- Hygroscopicity of dust particles, the ability to act as cloud condensation nuclei, depends on the mineralogical composition
- Fertilization of phytoplankton in oceans is linked to availability of soluble iron, i.e., to the mineral types of dust

Hematite Mass Fraction → Single Scattering Albedo Moosmüller et al., JGR (2012)

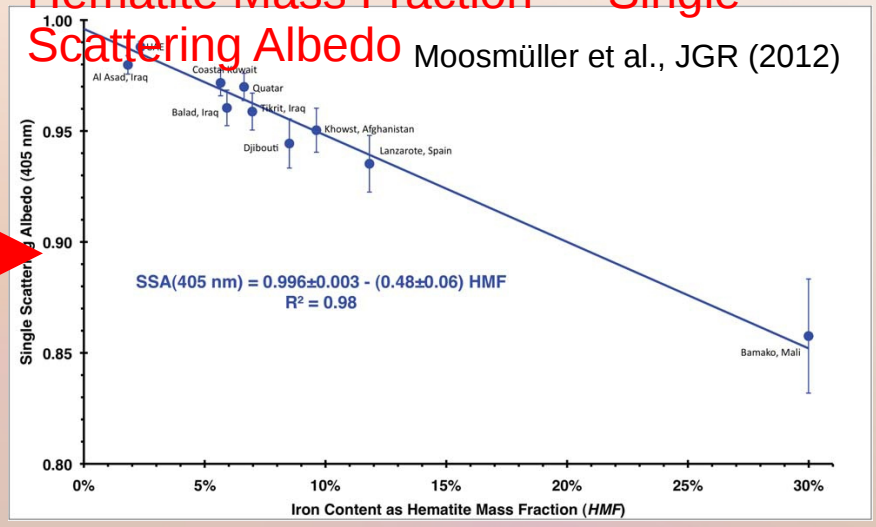

Perlwitz and Miller, JGR (2010),
Zonal Average 20º – 85º E in JJA:

More reflecting dust

More absorbing dust

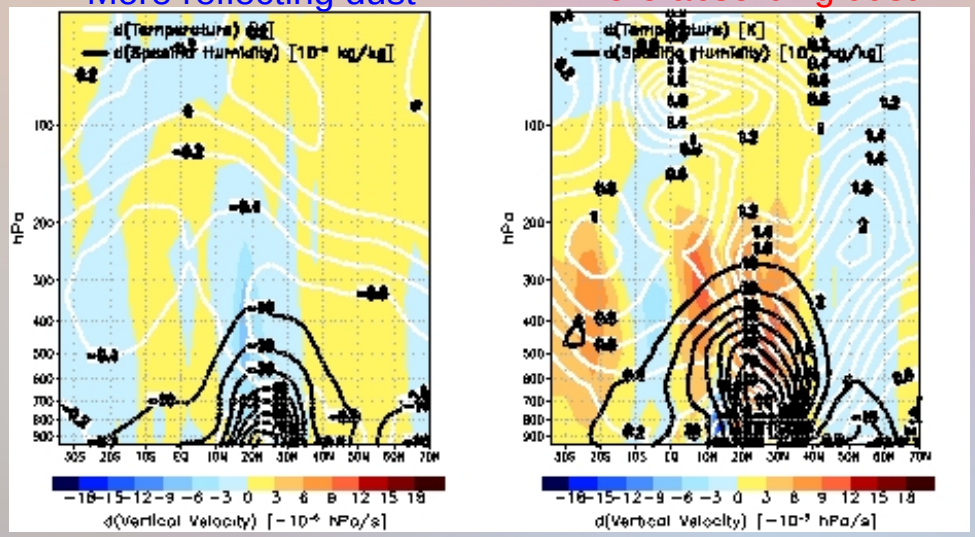

Shaded: Blue: Less Upward Red: More Upward

Hematite Content in Dust and Absorptivity

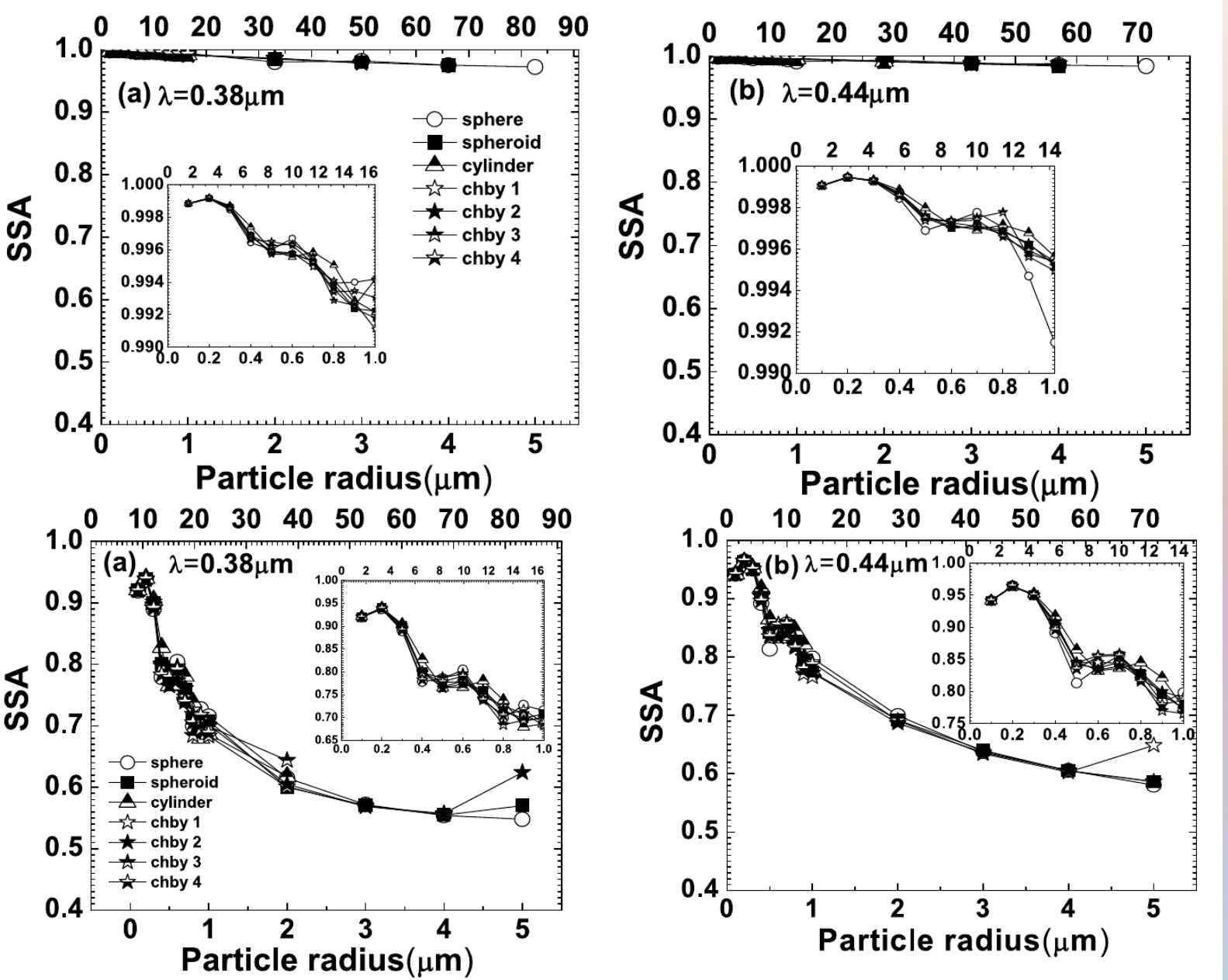

0%

2%

(Mishra and Tripathi, JGR 2008)

Hematite Content in Dust and Absorptivity

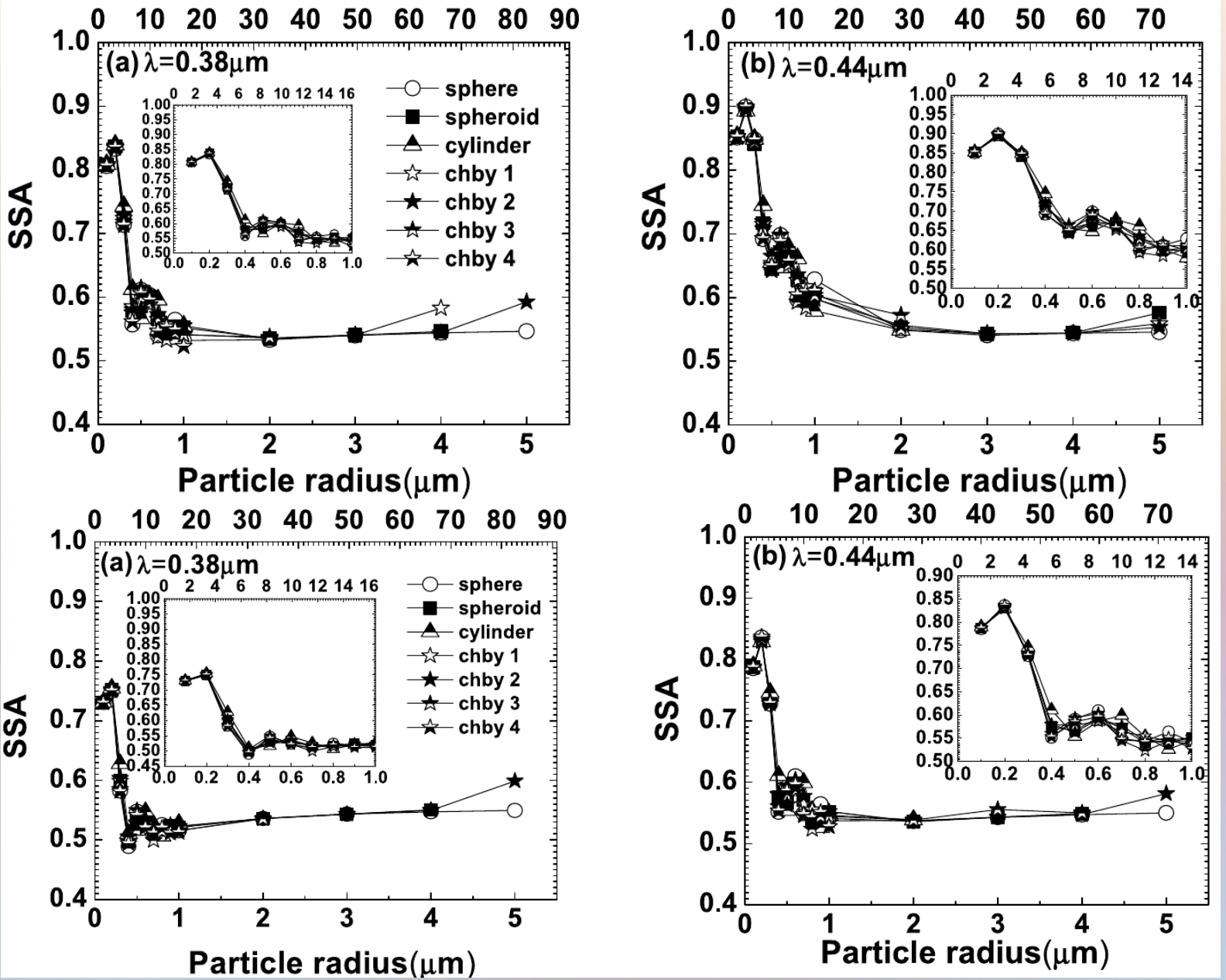

6%

10%

(Mishra and Tripathi, JGR 2008)

Why is the Mineral Composition of Soil Dust Important?

- Traditionally, global dust models have used globally uniform dust properties

Limitations for following reasons:

- Single scattering albedo (SSA) of dust particles depends on mineral composition, particularly on the mass fraction of hematite or goethite
- In turn, aerosol forcing and the response of clouds and atmospheric circulation to the forcing depend on the SSA
- Heterogenous chemistry (e.g., uptake rates) of dust particles depends on mineralogical and chemical composition
- Hygroscopicity of dust particles, the ability to act as cloud condensation nuclei, depends on the mineralogical composition
- Fertilization of phytoplankton in oceans is linked to availability of soluble iron, i.e., to the mineral types of dust

Hematite Mass Fraction → Single Scattering Albedo Moosmüller et al., JGR (2012)

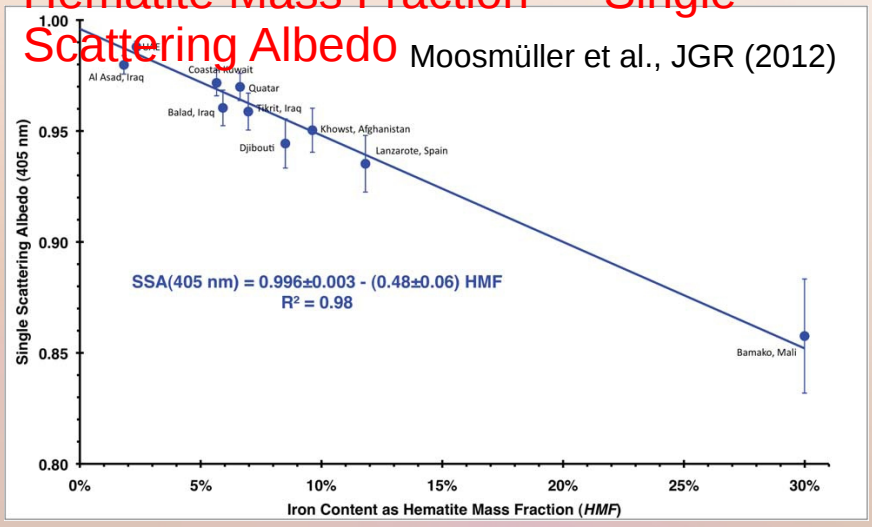

Perlwitz and Miller, JGR (2010),
Zonal Average 20º – 85º E in JJA:

More reflecting dust

More absorbing dust

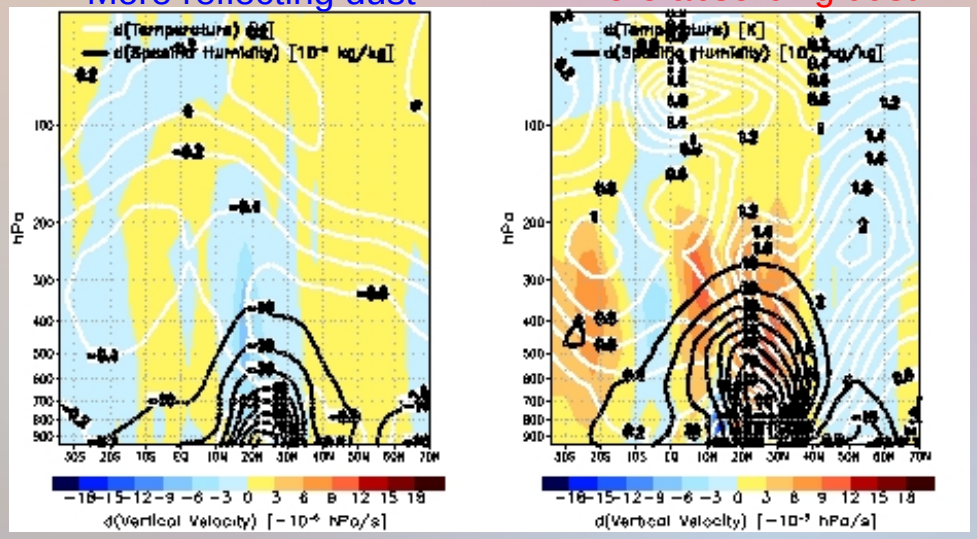

Shaded: Blue: Less Upward Red: More Upward

Why is the Mineral Composition of Soil Dust Important?

- Traditionally, global dust models have used globally uniform dust properties

Limitations for following reasons:

- Single scattering albedo (SSA) of dust particles depends on mineral composition, particularly on the mass fraction of hematite or goethite
- In turn, aerosol forcing and the response of clouds and atmospheric circulation to the forcing depend on the SSA
- Heterogenous chemistry (e.g., uptake rates) of dust particles depends on mineralogical and chemical composition
- Hygroscopicity of dust particles, the ability to act as cloud condensation nuclei, depends on the mineralogical composition
- Fertilization of phytoplankton in oceans is linked to availability of soluble iron, i.e., to the mineral types of dust

Hematite Mass Fraction → Single Scattering Albedo Moosmüller et al., JGR (2012)

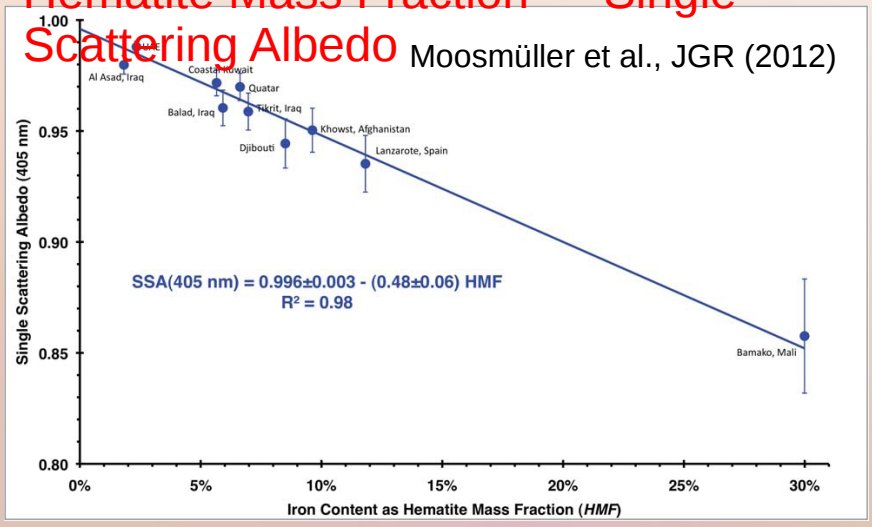

Perlwitz and Miller, JGR (2010),
Zonal Average 20º – 85º E in JJA:

More reflecting dust

More absorbing dust

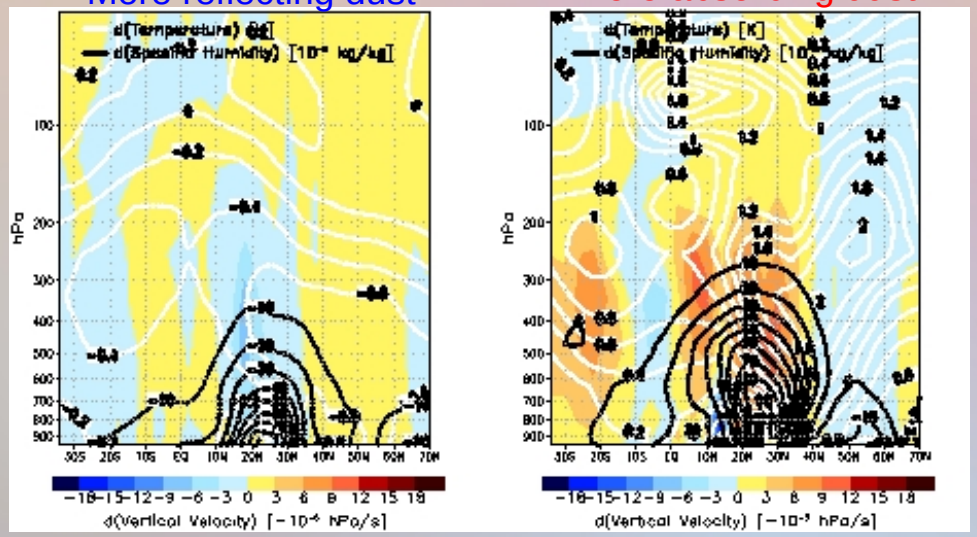

Shaded: Blue: Less Upward Red: More Upward

Why is the Mineral Composition of Soil Dust Important?

- Traditionally, global dust models have used globally uniform dust properties

Limitations for following reasons:

- Single scattering albedo (SSA) of dust particles depends on mineral composition, particularly on the mass fraction of hematite or goethite
- In turn, aerosol forcing and the response of clouds and atmospheric circulation to the forcing depend on the SSA
- Heterogenous chemistry (e.g., uptake rates) of dust particles depends on mineralogical and chemical composition
- Hygroscopicity of dust particles, the ability to act as cloud condensation nuclei, depends on the mineralogical composition
- Fertilization of phytoplankton in oceans is linked to availability of soluble iron, i.e., to the mineral types of dust

Hematite Mass Fraction → Single Scattering Albedo Moosmüller et al., JGR (2012)

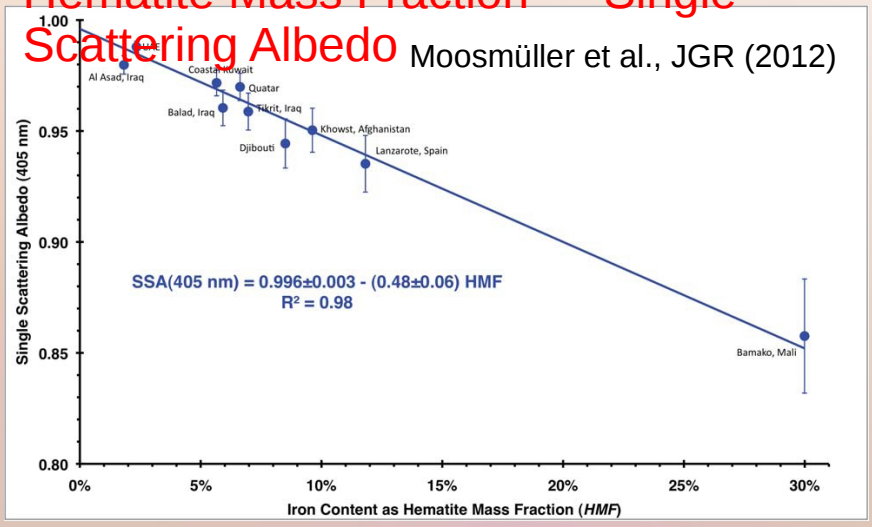

Perlwitz and Miller, JGR (2010),
Zonal Average 20º – 85º E in JJA:

More reflecting dust

More absorbing dust

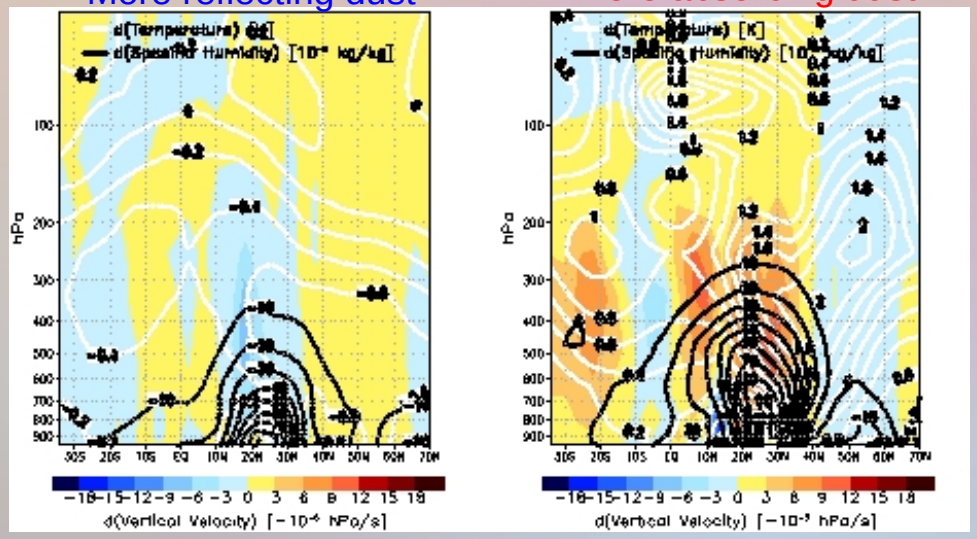

Shaded: Blue: Less Upward Red: More Upward

Why is the Mineral Composition of Soil Dust Important?

- Traditionally, global dust models have used globally uniform dust properties

Limitations for following reasons:

- Single scattering albedo (SSA) of dust particles depends on mineral composition, particularly on the mass fraction of hematite or goethite
- In turn, aerosol forcing and the response of clouds and atmospheric circulation to the forcing depend on the SSA
- Heterogenous chemistry (e.g., uptake rates) of dust particles depends on mineralogical and chemical composition
- Hygroscopicity of dust particles, the ability to act as cloud condensation nuclei, depends on the mineralogical composition
- Fertilization of phytoplankton in oceans is linked to availability of soluble iron, i.e., to the mineral types of dust

Hematite Mass Fraction → Single Scattering Albedo Moosmüller et al., JGR (2012)

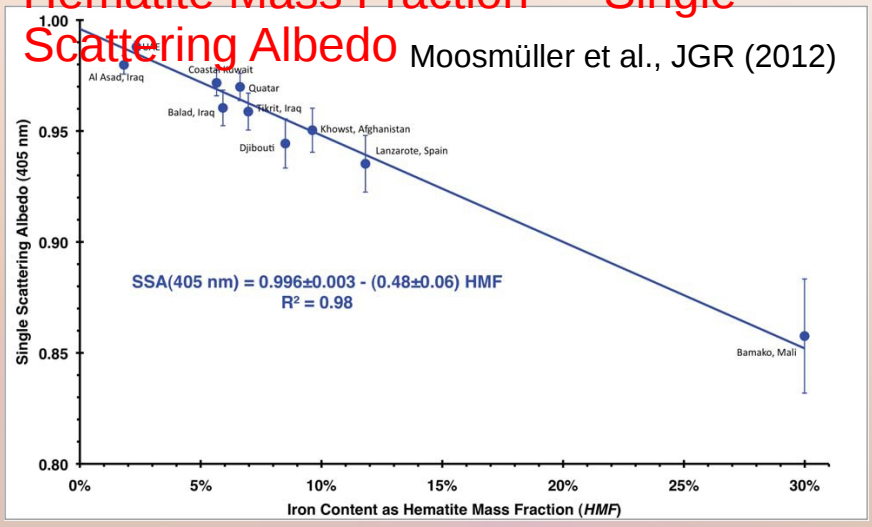

Perlwitz and Miller, JGR (2010),
Zonal Average 20º – 85º E in JJA:

More reflecting dust

More absorbing dust

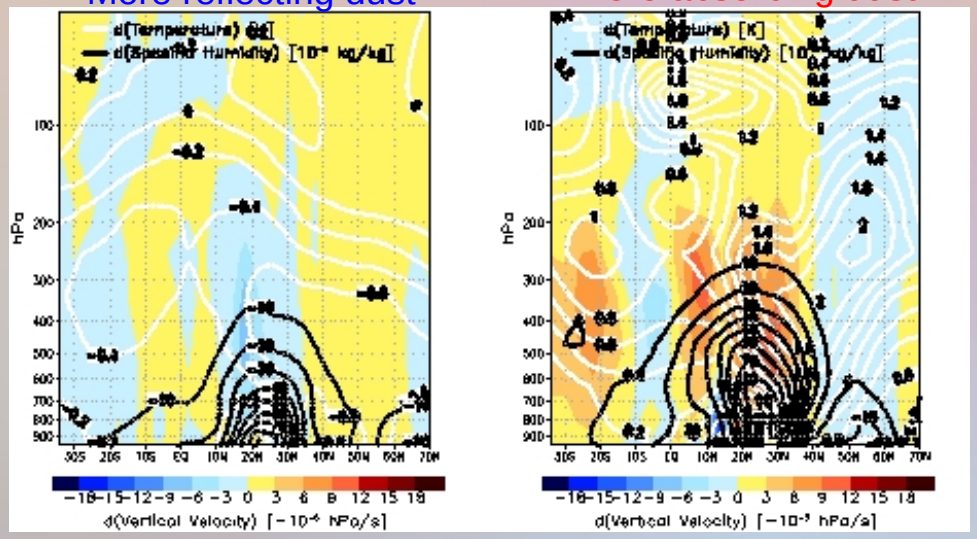

Shaded: Blue: Less Upward Red: More Upward

New Soil Dust in NASA-GISS ModelE2 With Mineralogy

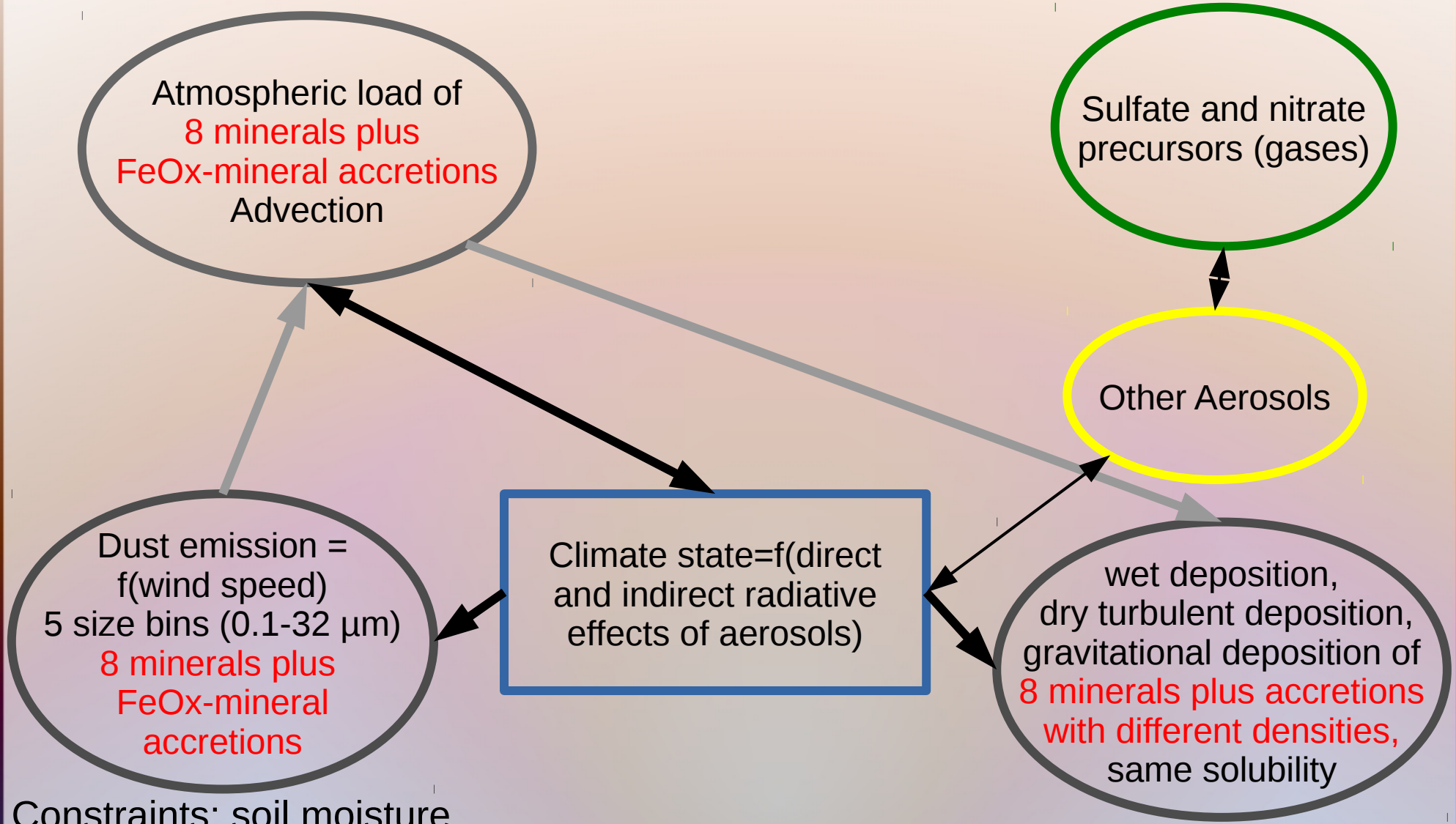

Constraints: soil moisture, vegetation cover, (land use), size dependent mineral composition of soils

New Soil Dust in NASA-GISS ModelE2 With Mineralogy

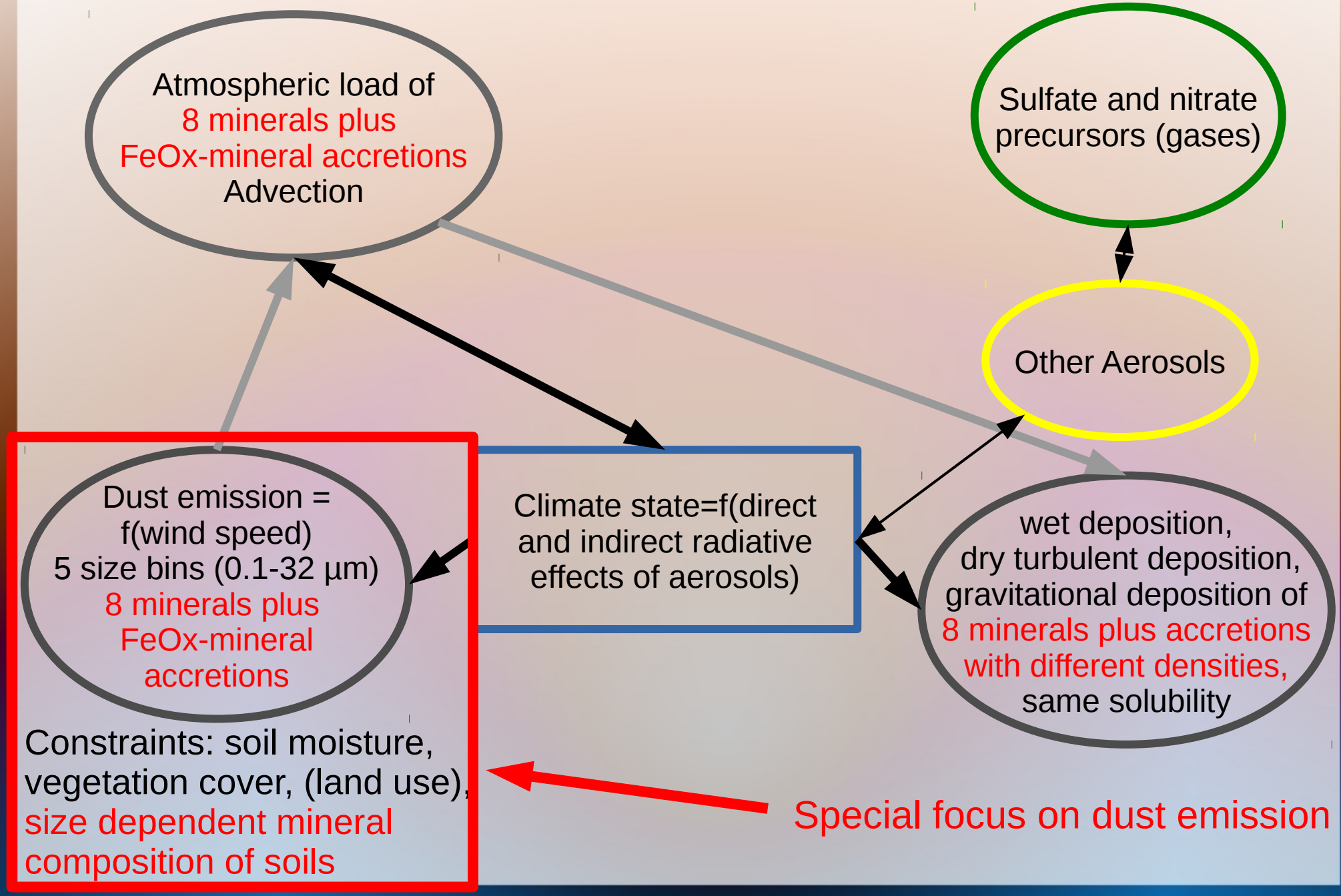

The Main Data Sets Needed

1. Mean Mineralogical Table (MMT) by Claquin et al., JGR (1999) + Nickovic et al., ACP (2012)

The mineralogical composition of soils varies with the soil type. The MMT provides this information for 28 arid soil types

Table 2. Mean Mineralogy Table

Soil Types	Clay Fraction Ill	Kao	Sme	Cal	Qua	Silt Fraction Qua	Fel	Cal	Hem	Gyp	N	A
Lithosols I												
Average	40	20	29	4	7	53	40	6	1	1	6	7
s.d.	13	18	17	4	3	14	12	6	1	1		
Calcic Fluvisols Jc												
Average	22	9	46	11	12	31	39	30	0	2	10	2
s.d.	4	3	13	2	3	2	4	3	0	1		
Eutric Fluvisols Je												
Average	18	23	55	1	3	86	10	2	1	1	12	1
s.d.	10	11	19	1	2	13	5	2	1	1		
Sand Dunes SD												
Average	50	9	26	1	14	92	6	1	1	1	8	12
s.d.	12	5	6	1	4	3	3	1	1	1		
Salt Flats ST												
Average	39	4	26	29	1	5	1	93	1	26	14	3
s.d.	12	3	18	3	1	4	1	27	1	10		

An updated table has just been published by Journet et al. ACP (2014), which is not used here.

2. Digital Soil Map of the World (DSMW) (FAO-UNESCO, 2007)

Geographical distribution of dominant top soil types
(5'x5' latitude by longitude)

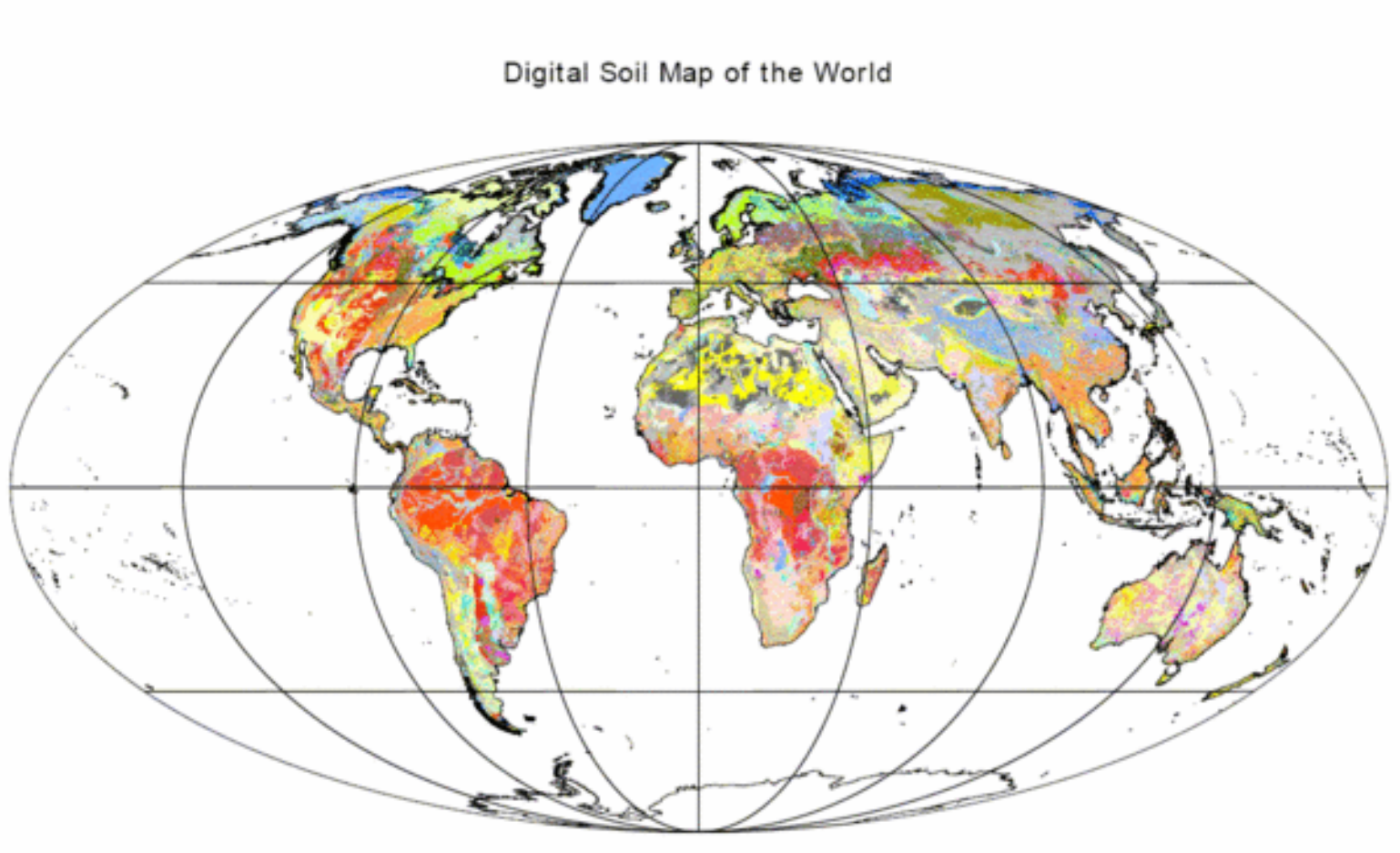

3. FAO/STATSGO Soil Texture Fractions

Geographical distribution of clay, silt, and sand fraction for soil texture types (5'x5' latitde by longitude)

Class No.	Soil texture class	Sand [%]	Silt [%]	Clay [%]
1	Sand	92	5	3
2	Loamy Sand	82	12	6
3	Sandy Loam	58	32	10
4	Silt Loam	17	70	13
5	Silt	10	85	5
6	Loam	43	39	18
7	Sandy Clay Loam	58	15	27
8	Silty Clay Loam	10	56	34
9	Clay Loam	32	34	34
10	Sandy Clay	52	6	42
11	Silty Clay	6	47	47
12	Clay	22	20	58

Fully dispersed soils!

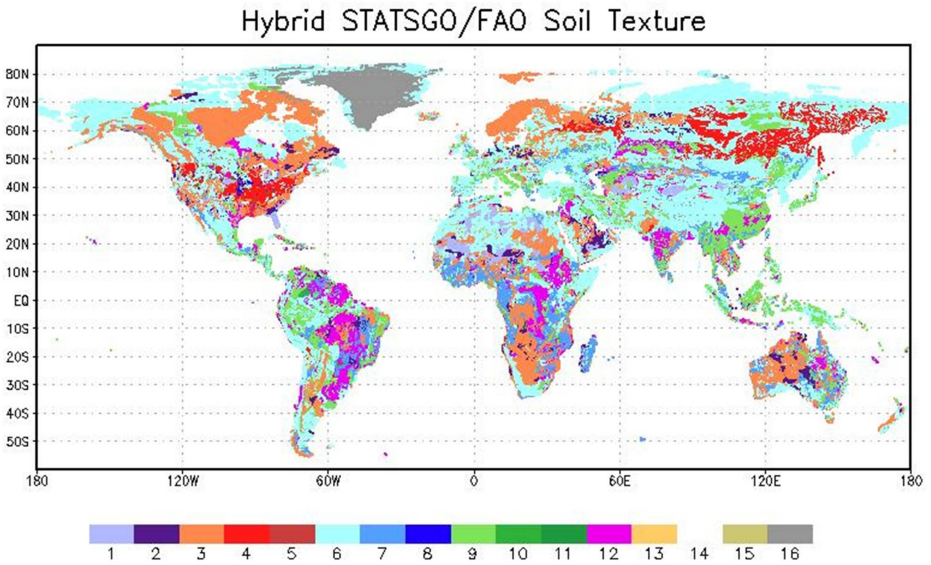

Figure source: http://ldas.gsfc.nasa.gov/gldas/GLDASsoils.php

How to Obtain the Emitted Mineral Fractions?

The Simple Approach. Case 1 - Soil Mineral Fraction (SMF) Method

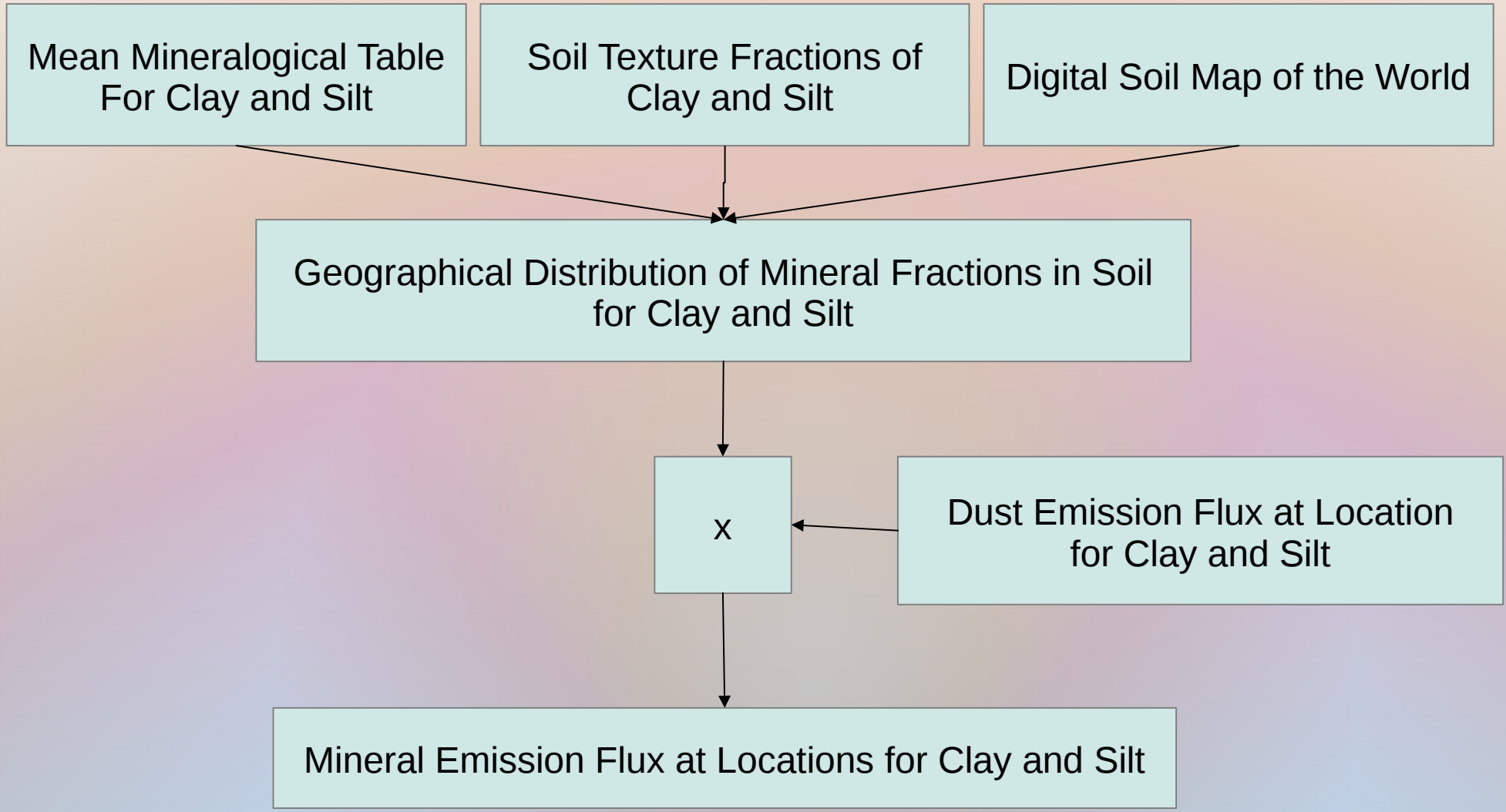

Challenge: Emission of Minerals from Soils

Previous dust models with mineralogy have assumed 1 to 1 translation of mineral fractions in soil data sets to mineral fractions of dust aerosols

Emission from Soils: Aggregated and Fragmented Dust Particles

Shao et al. (2011)

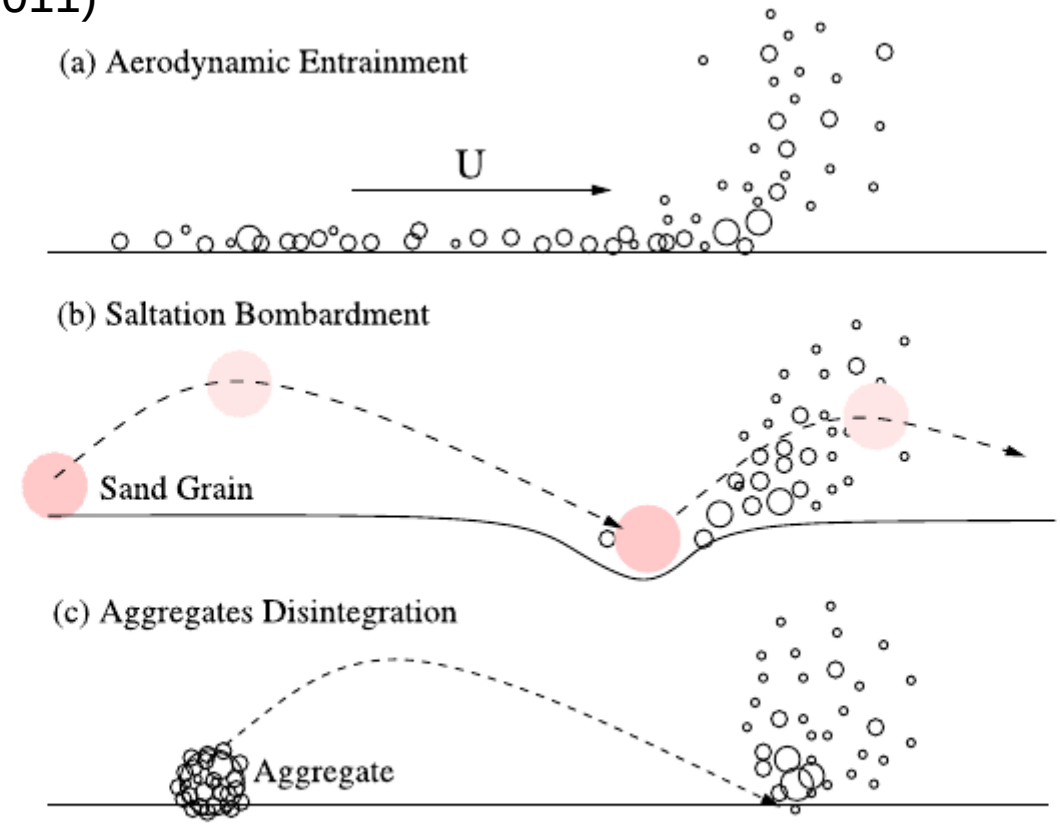

Figure 1. Mechanisms for dust emission. (a) F_a, dust emission by aerodynamic lift; (b) F_b, by saltation bombardment (sand blasting); and (c) F_c, through disaggregation of aggregates or fragments (self-abrasion).

Soil Texture and Mineral Fractions Determined Using Techniques Leading to Nearly Full Destruction of Aggregates

Figure 5-5. Laboratory sieves for mechanical analysis of grain size distribution. Shown (right to left) are sieve Nos. 3/8-in. (9.5-mm), No. 10 (2.0-mm), No. 40 (250-µm) and No. 200 (750-µm) and example soil particle sizes including (right to left): medium gravel, fine gravel, medium-coarse sand, silt, and dry clay (kaolin).

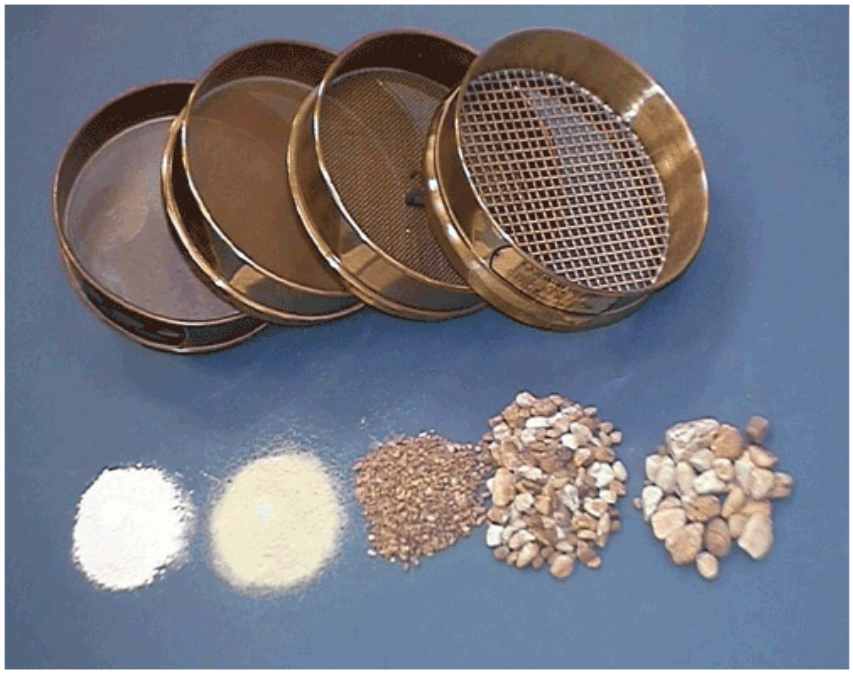

Figure 5-6. Soil hydrometer apparatus (http://www.ce.siue.edu/).

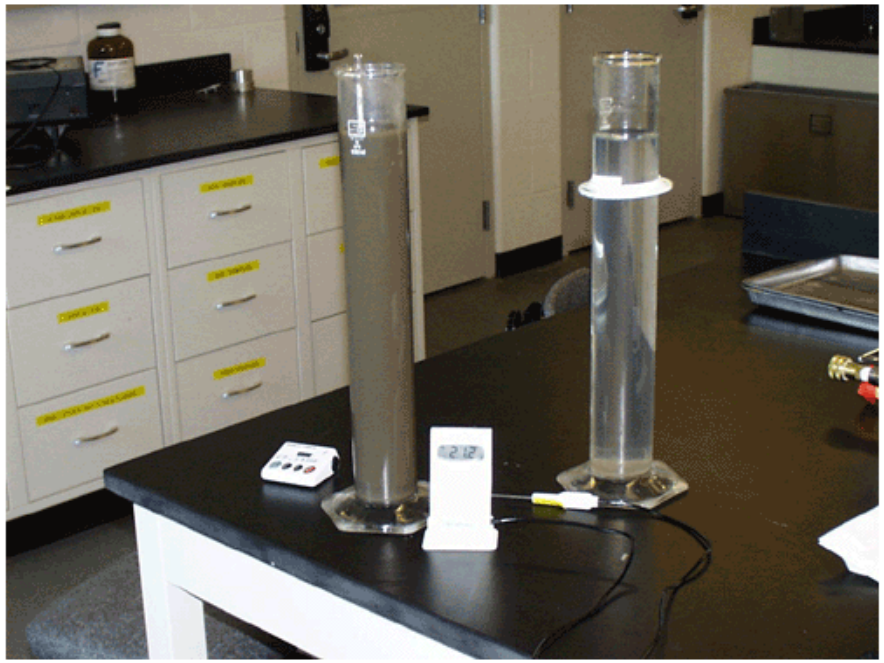

Source: http://www.fhwa.dot.gov/engineering/geotech/pubs/05037/05a.cfm

Wet Sieved Soil Texture Fractions ≠ Size Distribution of Eroded Soils

Wet Sieved Soil Texture Fractions ≠ Suspended Dust Size Distribution

Wet Sieved Clay/Silt Mineral Fractions ≠ Mineral Fractions of Suspended Dust

Mineral Fractions in Dust vs. Mean Mineralogical Table

Abundance of mineral groups over particle size at Tinfou, Morocco:

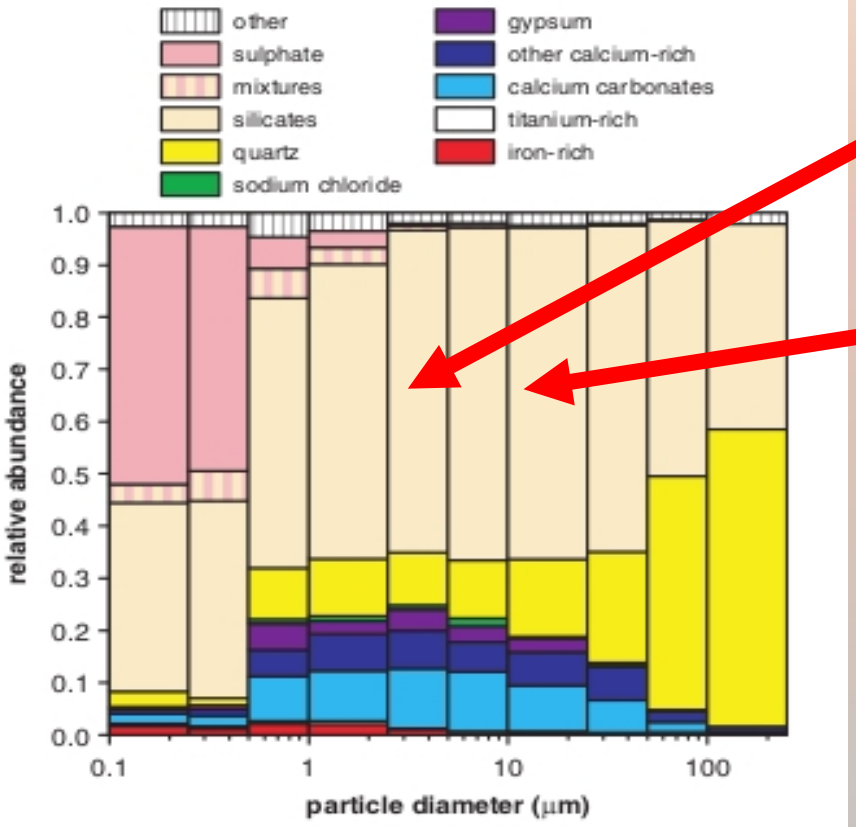

Fig. 11. Average relative volume abundance of the different particle classes at Tinfou ground station.

Kandler et al., Tellus B (2009)

- Significant Fractions of so called "Clays" like illite and kaolinite are being found in silt size range, but missing in silt size range of MMT
- Silicates can even have the largest fraction in silt size range.
- Quartz may be dominant only for largest sizes.
- Feldspar, gypsum missing in clay size range of MMT

Another challenge with MMT:
No accretions of iron oxides! Iron oxides have higher density than other minerals and fall out faster. How are they transported in the model?

Mineral Fractions in Dust vs. Mean Mineralogical Table

Abundance of mineral groups over particle size at Tinfou, Morocco:

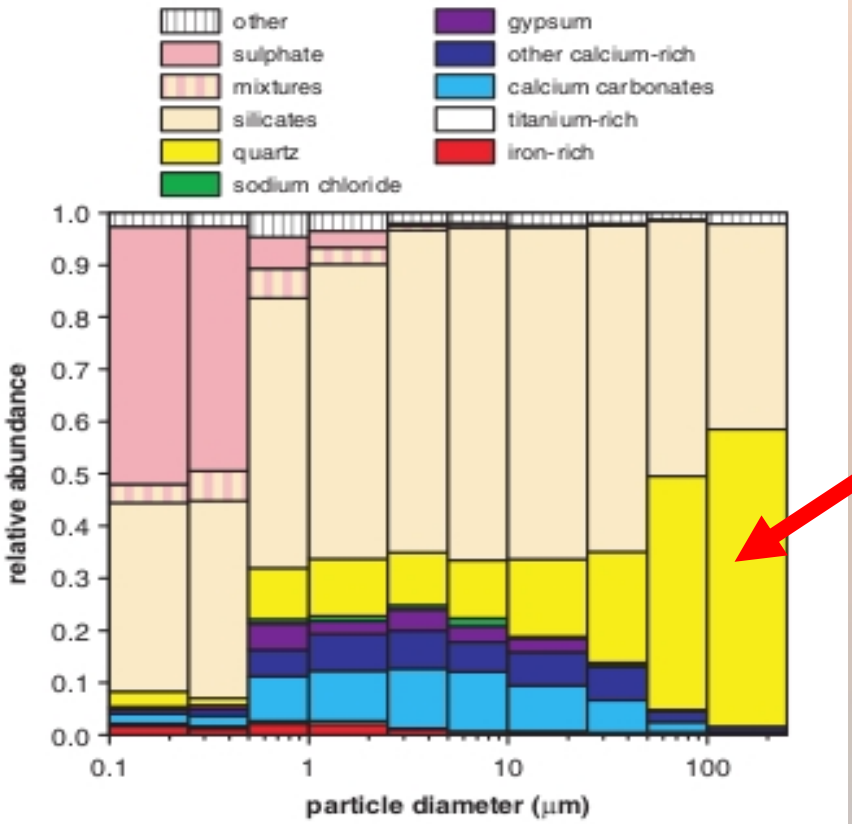

Fig. 11. Average relative volume abundance of the different particle classes at Tinfou ground station.

Kandler et al., Tellus B (2009)

- Significant Fractions of so called “Clays” like illite and kaolinite are being found in silt size range, but missing in silt size range of MMT
- Silicates can even have the largest fraction in silt size range.
- Quartz may be dominant only for largest sizes.
- Feldspar, gypsum missing in clay size range of MMT

Another challenge with MMT:
No accretions of iron oxides! Iron oxides have higher density than other minerals and fall out faster. How are they transported in the model?

Mineral Fractions in Dust vs. Mean Mineralogical Table

Abundance of mineral groups over particle size at Tinfou, Morocco:

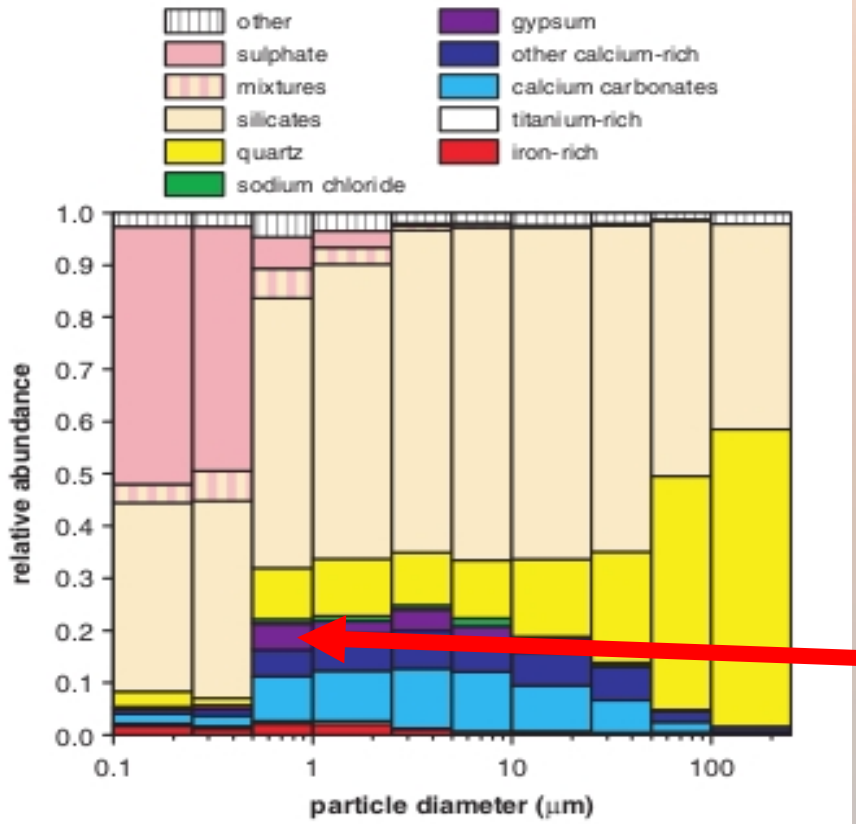

Fig. 11. Average relative volume abundance of the different particle classes at Tinfou ground station.

Kandler et al., Tellus B (2009)

- Significant Fractions of so called “Clays” like illite and kaolinite are being found in silt size range, but missing in silt size range of MMT
- Silicates can even have the largest fraction in silt size range.
- Quartz may be dominant only for largest sizes.
- Feldspar, gypsum missing in clay size range of MMT

Another challenge with MMT:
No accretions of iron oxides! Iron oxides have higher density than other minerals and fall out faster. How are they transported in the model?

Mineral Fractions in Dust vs. Mean Mineralogical Table

Abundance of mineral groups over particle size at Tinfou, Morocco:

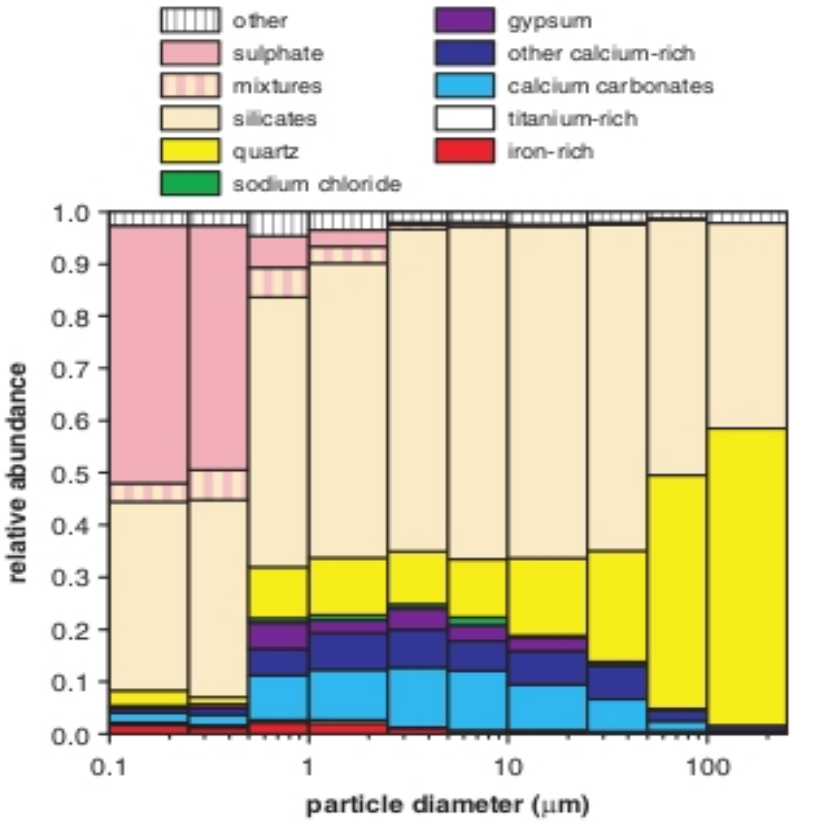

Fig. 11. Average relative volume abundance of the different particle classes at Tinfou ground station.

Kandler et al., Tellus B (2009)

- Significant Fractions of so called “Clays” like illite and kaolinite are being found in silt size range, but missing in silt size range of MMT
- Silicates can even have the largest fraction in silt size range.
- Quartz may be dominant only for largest sizes.
- Feldspar, gypsum missing in clay size range of MMT

Another challenge with MMT:
No accretions of iron oxides! Iron oxides have higher density than other minerals and fall out faster. How are they transported in the model?

Normalized Volume Size Distribution of Mineral Fractions in Dust Derived From Data Provided by Kandler et al. Tellus B (2009)

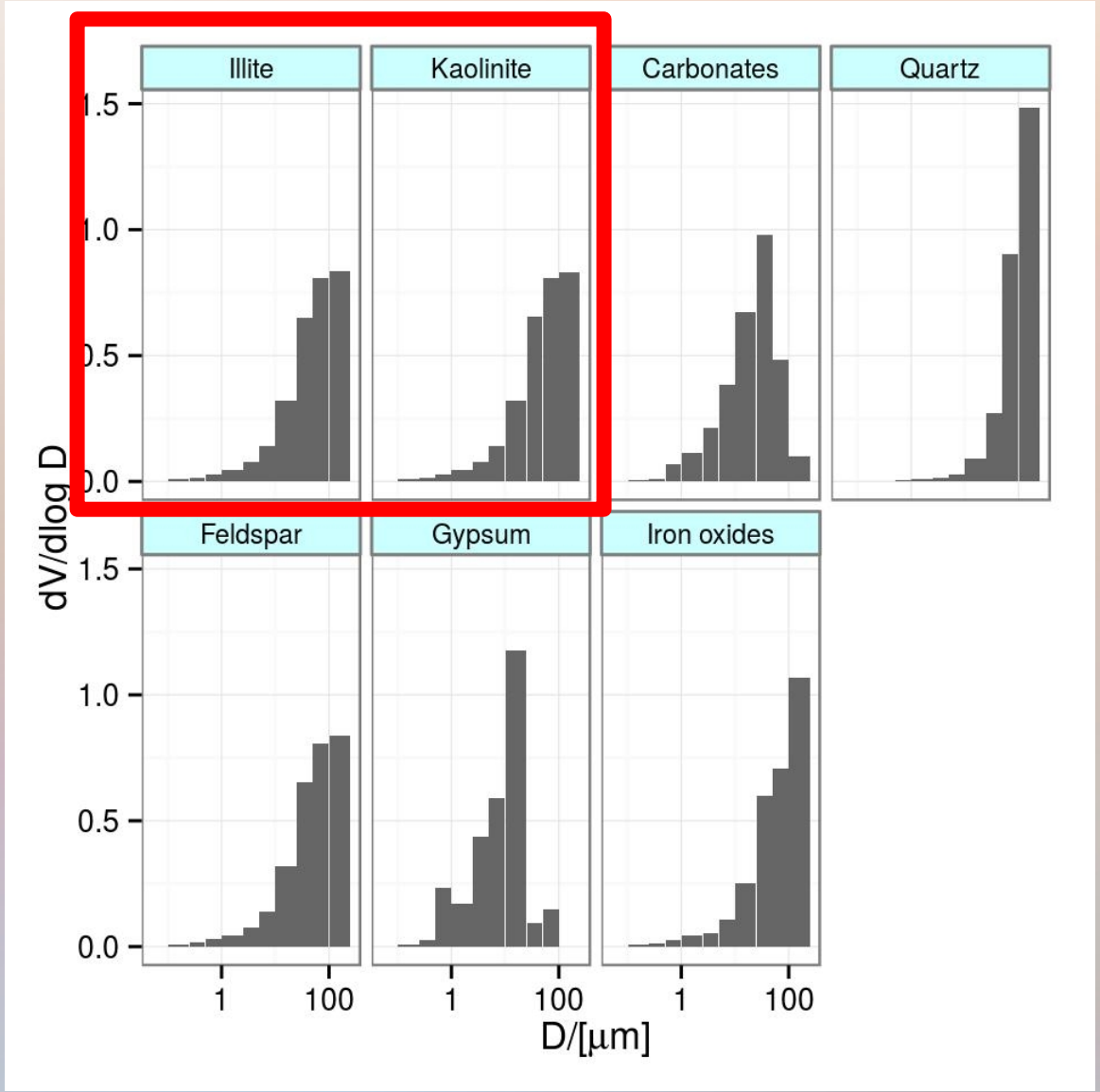

- Illite and kaolinite: Similar volume size distribution; most of the volume (mass) is found in higher particle size classes, even beyond silt size range (probably mostly due to aggregation)
- The carbonates and gypsum peak in the coarse silt size class
- Distinctive size distribution of quartz with steep increase in the volume distribution for largest particle sizes

Normalized Volume Size Distribution of Mineral Fractions in Dust Derived From Data Provided by Kandler et al. Tellus B (2009)

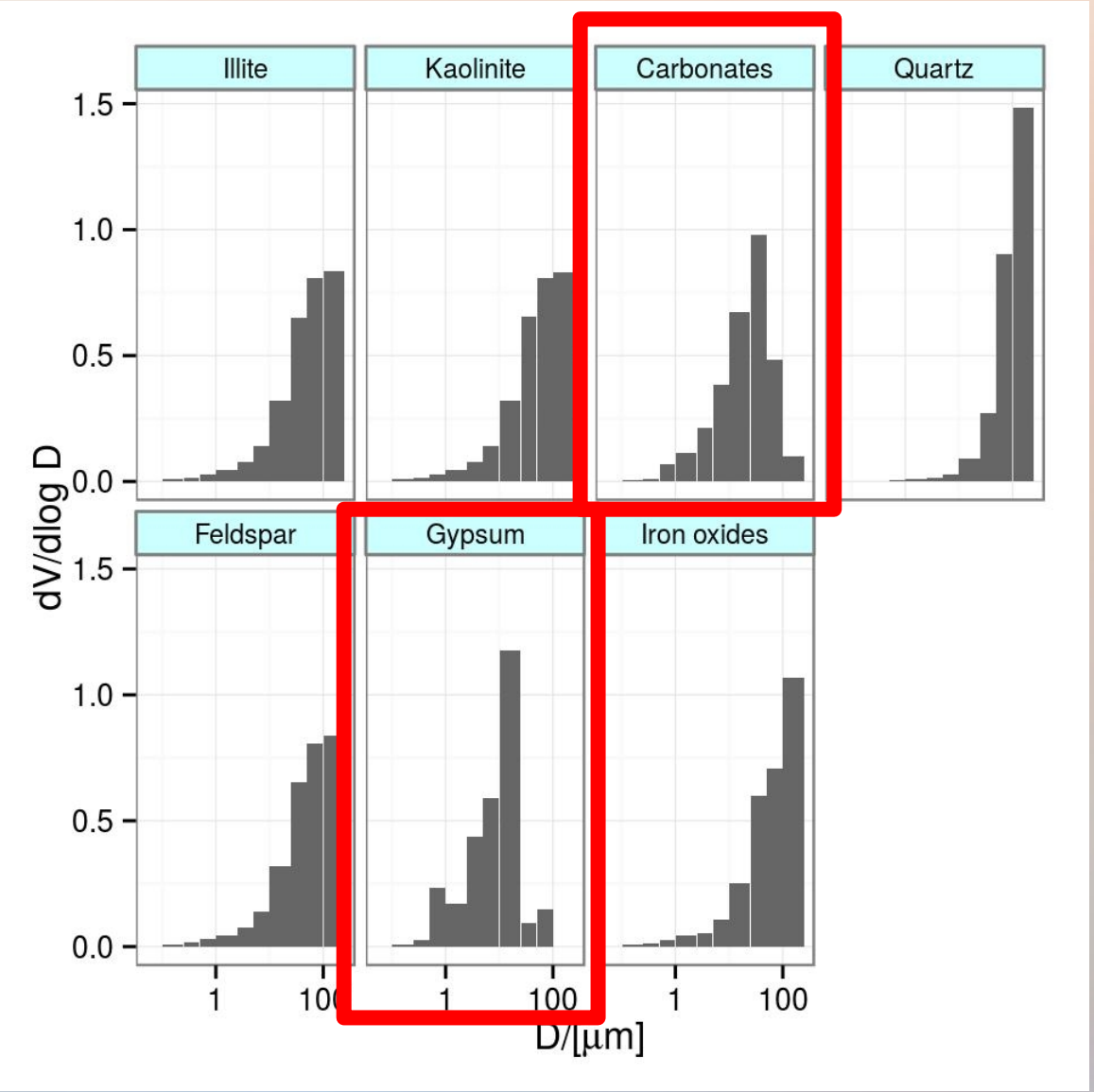

- Illite and kaolinite: Similar volume size distribution; most of the volume (mass) is found in higher particle size classes, even beyond silt size range (probably mostly due to aggregation)
- The carbonates and gypsum peak in the coarse silt size class
- Distinctive size distribution of quartz with steep increase in the volume distribution for largest particle sizes

Normalized Volume Size Distribution of Mineral Fractions in Dust Derived From Data Provided by Kandler et al. Tellus B (2009)

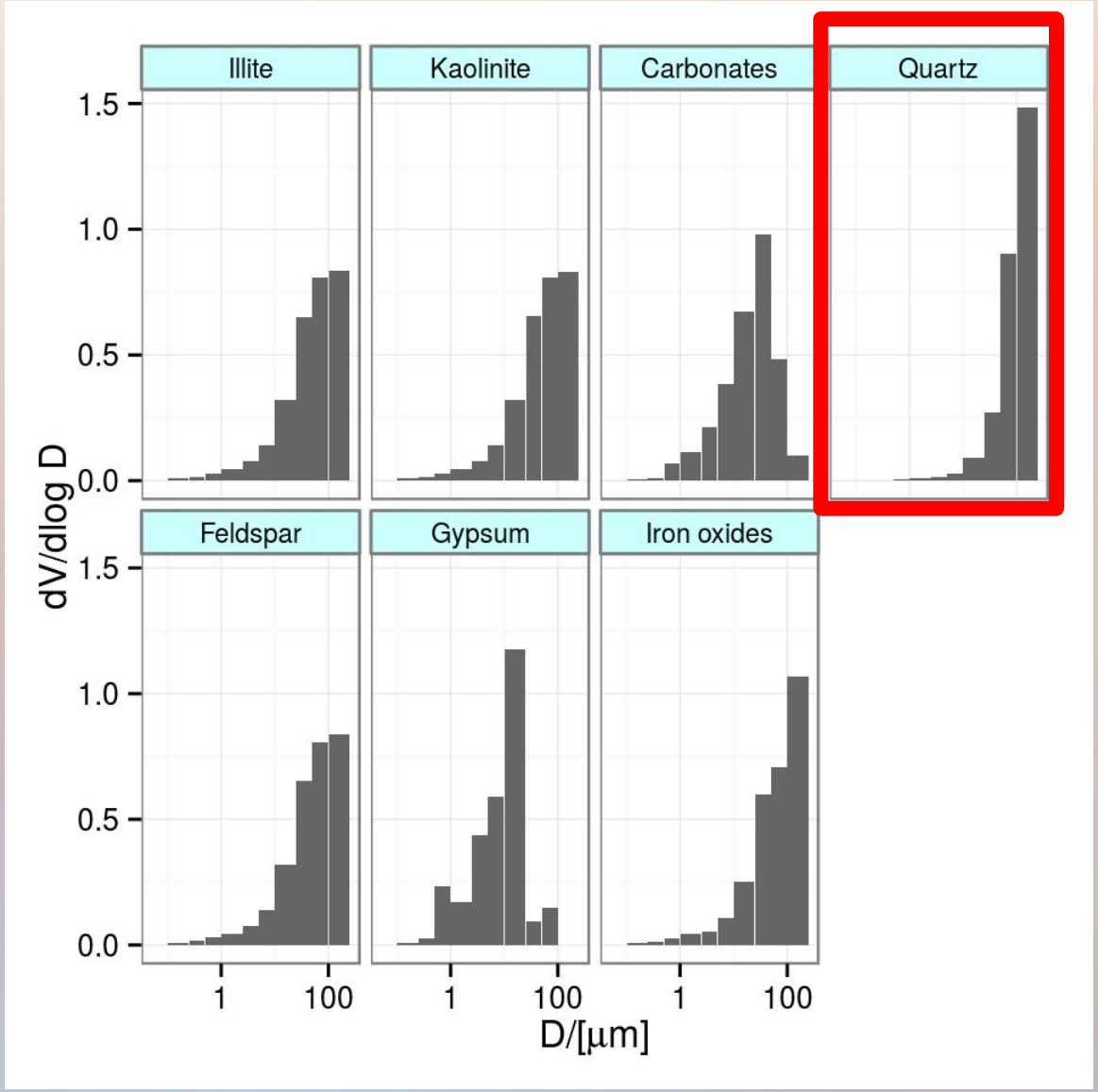

- Illite and kaolinite: Similar volume size distribution; most of the volume (mass) is found in higher particle size classes, even beyond silt size range (probably mostly due to aggregation)
- The carbonates and gypsum peak in the coarse silt size class
- Distinctive size distribution of quartz with steep increase in the volume distribution for largest particle sizes

Aerosol Mineral Fraction (AMF) Method

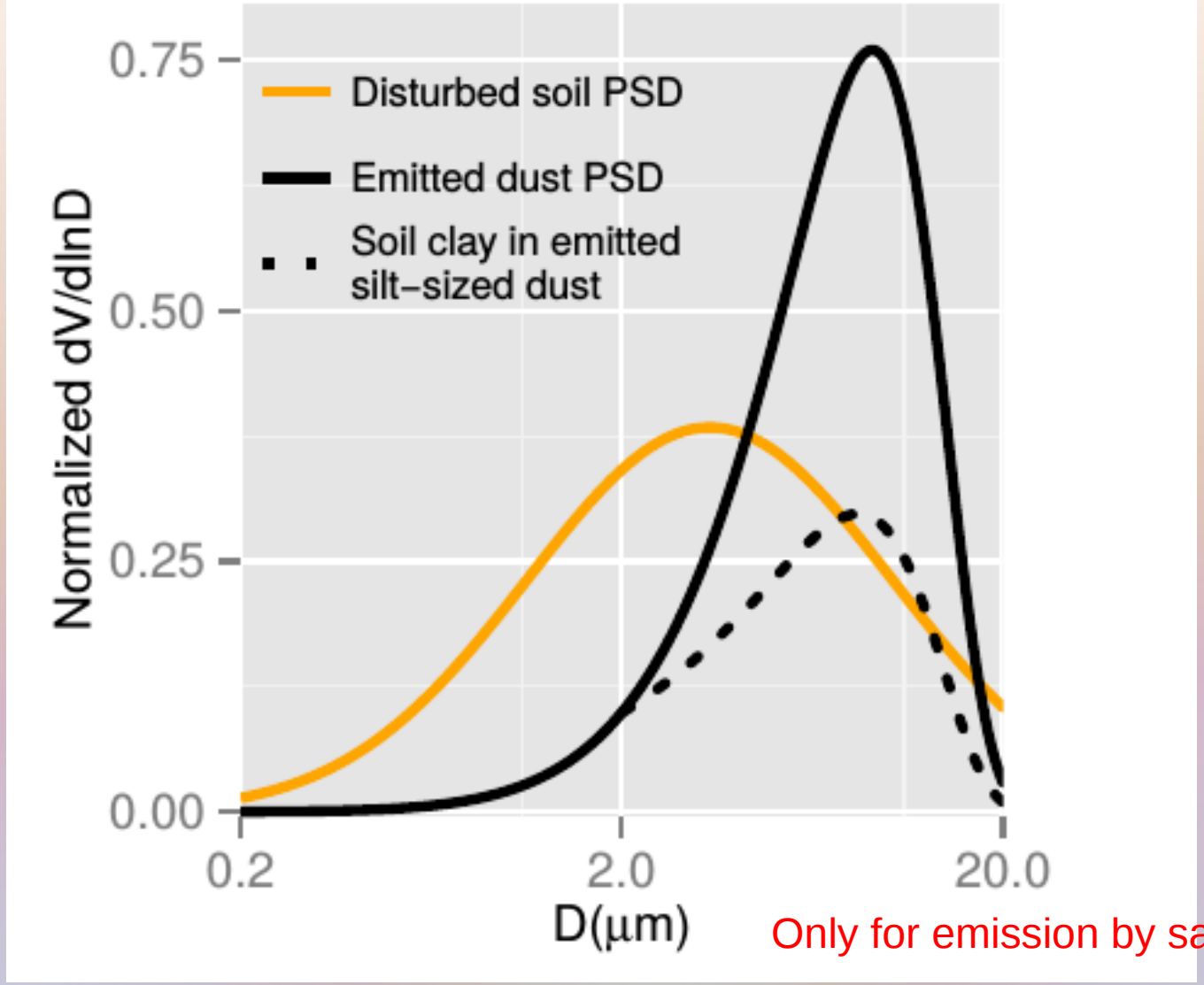

Only for emission by saltation!

Fully disbursed mineral mass in soil → Re-aggregation → Reconstructed size-dependent mineral mass in aerosols

Perlwitz et al., ACPD (2015a)

Brittle fragmentation theory (Kok, PNAS 2011)

Volume Size Distribution of Emitted Minerals in ModelE2

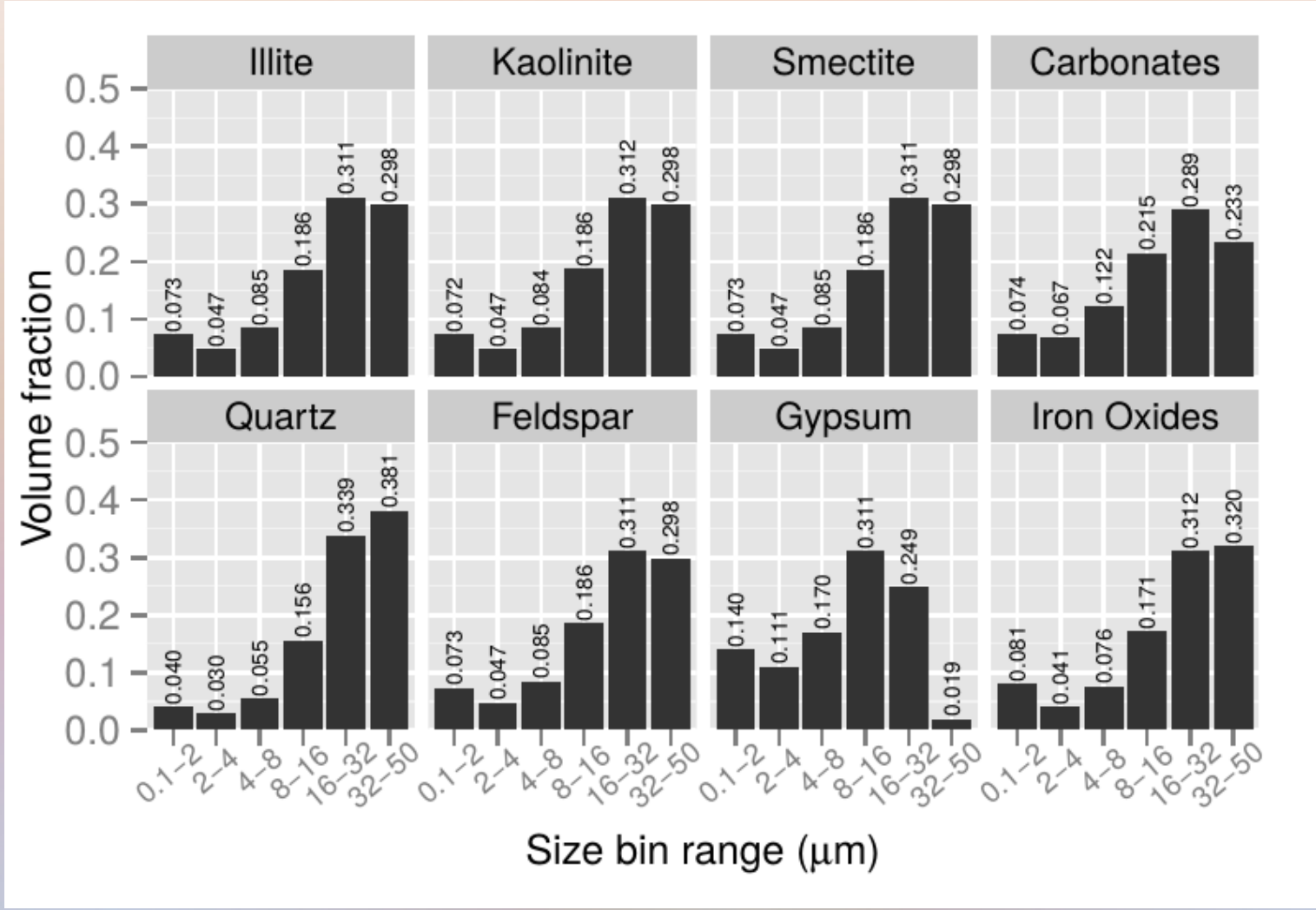

Perlwitz et al., ACPD (2015a)

Surface Concentration of Total Dust

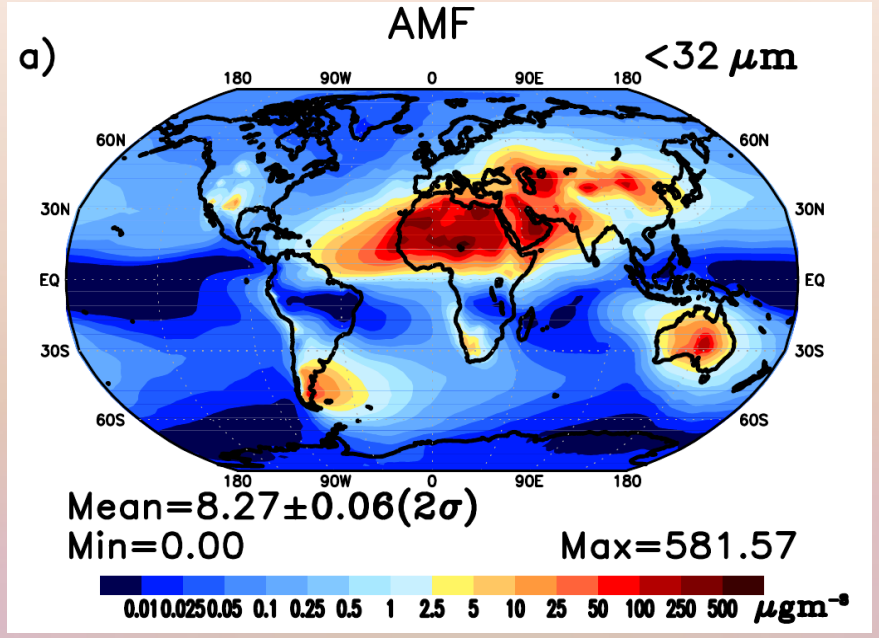

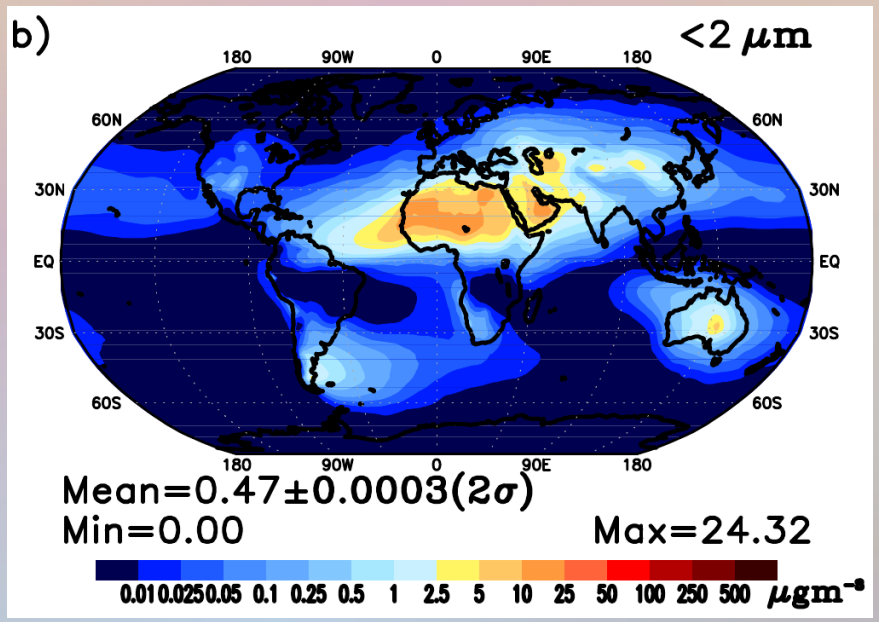

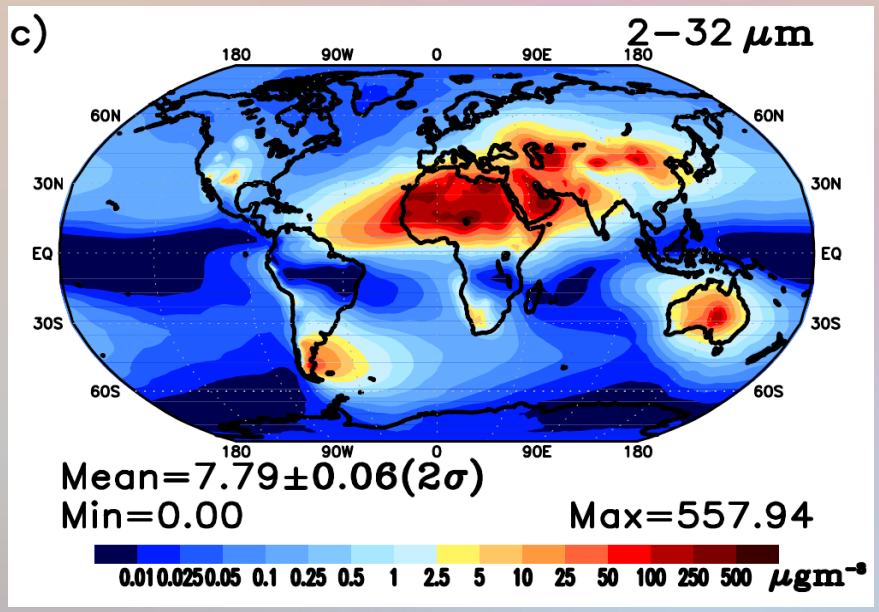

Simulated Mineral Fractions of Dust Column Mass

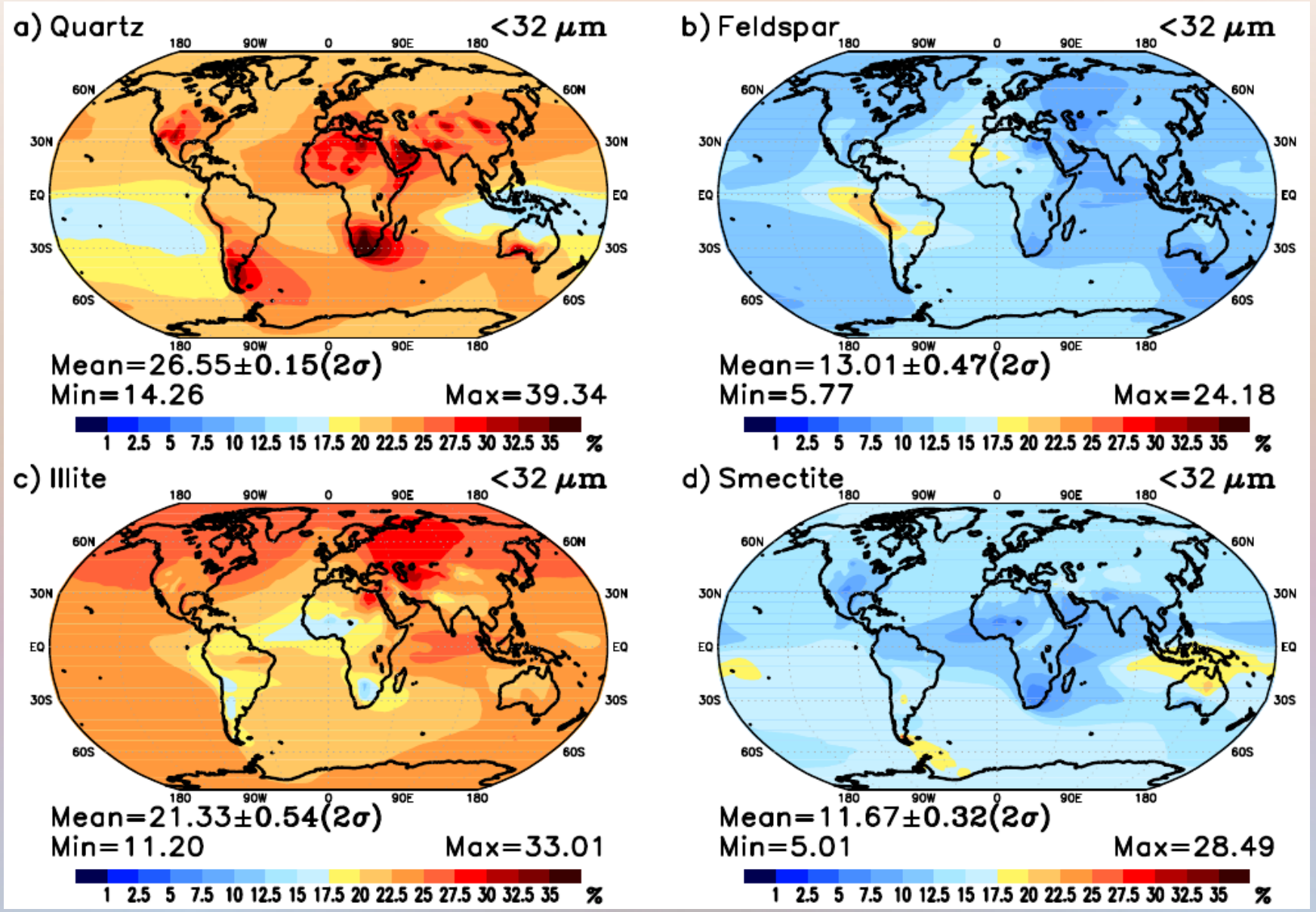

Simulated Mineral Fractions of Dust Column Mass

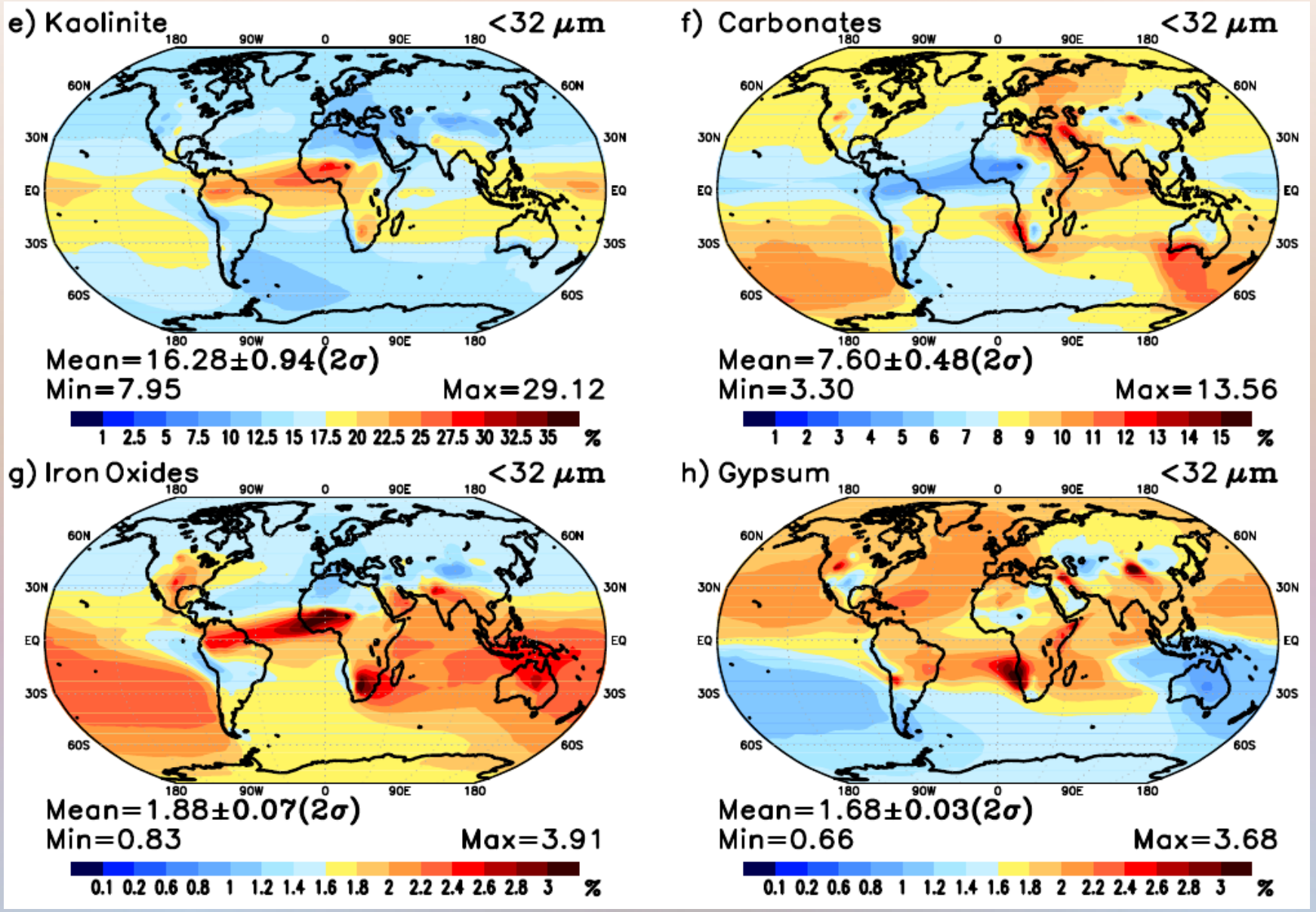

Iron Oxide Accretions With Other Minerals

Non-accreted mineral fractions at emission

ASSUMPTION: Accretion Probability: P=f(M)x(1-f(Fe-ox))

Operations (done in GCM)

Accretions of iron oxides with each of the other minerals

Non-accreted iron oxides

Non-accreted other minerals

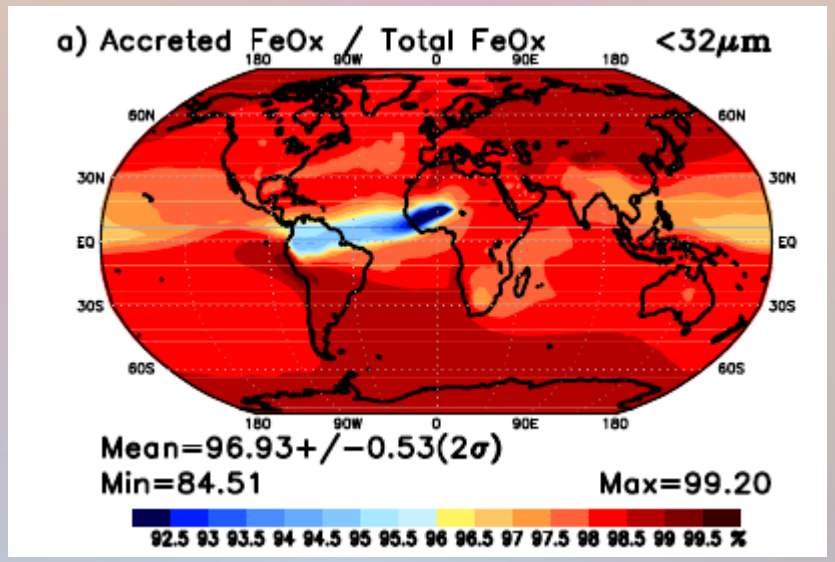

Almost all of iron oxide mass accreted

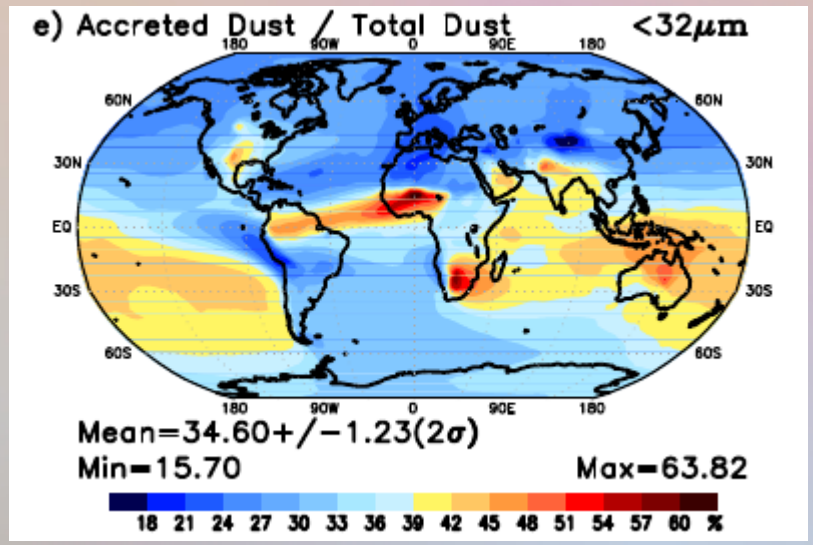

About 35% of non-FeOx dust with FeOx impurities

Evaluation

- Compilation of about 60 references from literature with mineral fraction measurements (Perlwitz et al., ACPD 2015b)
- Limitations: Mostly campaign data or cruises, small sampling size, possible biases depending on the methods; How to compare to model climatology?

Locations of Measurements from Literature

Perlwitz et al., ACPD (2015b)

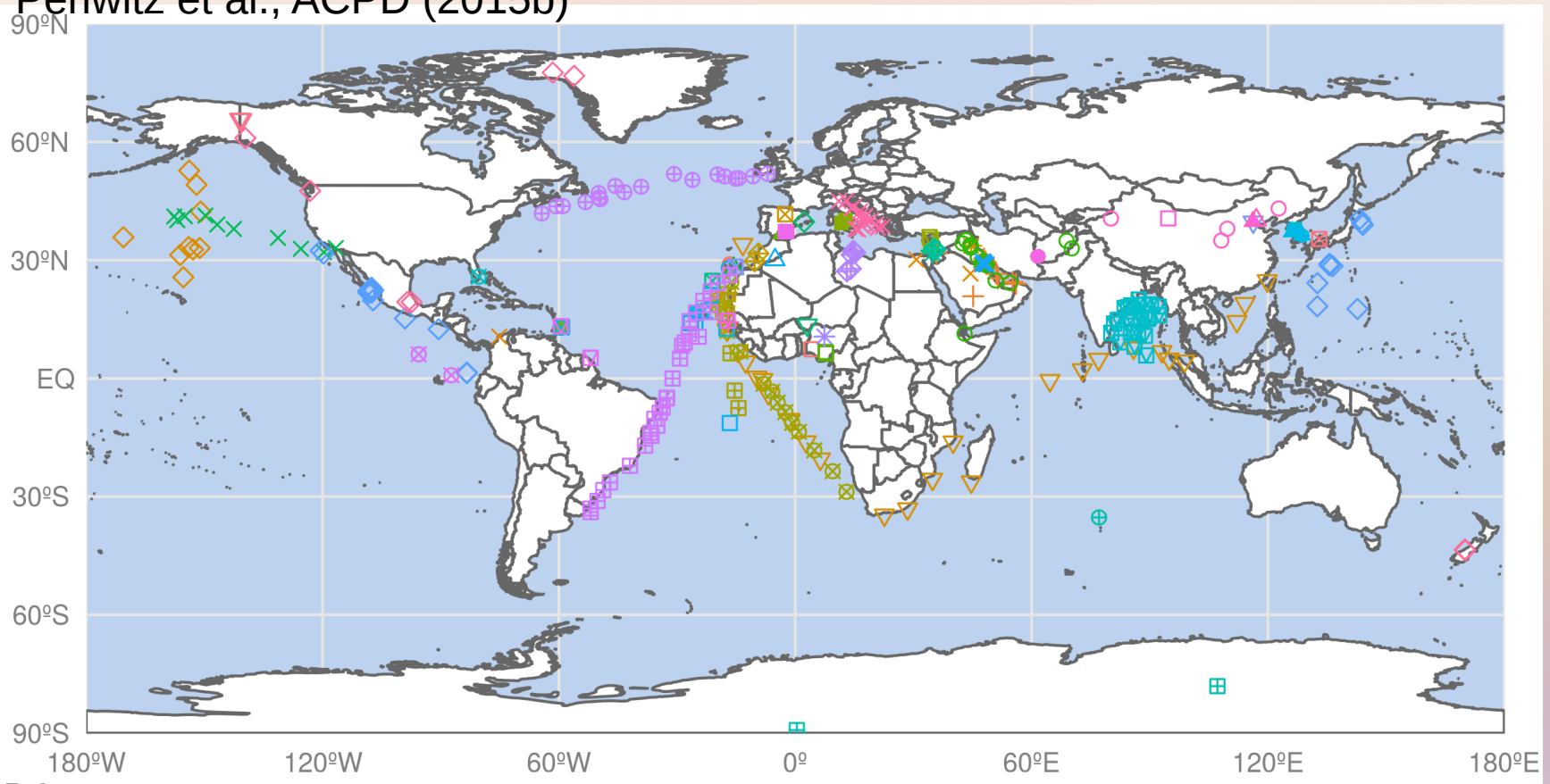

Reference

- Adedokum et al. (1989):7.29ºN,4.34ºE
- Alastuey et al. (2005)
- Al-Awadhi and AlShuaibi (2013)
- Al-Dousari and Al-Awadhi (2012)
- Al-Dousari et al. (2013)
- Arnold et al. (1998)
- Aston et al. (1973)
- Avila et al. (1997):41.77ºN,2.35ºW
- Awadh (2012):33.33ºN,44.43ºE
- Chester and Johnson (1971a)
- Chester and Johnson (1971b)
- Chester et al. (1971)
- Chester et al. (1972)
- Chester et al. (1977)
- Chester et al. (1984)
- Delany et al. (1967):13.17ºN,59.42ºW
- Díaz-Hernández et al. (2011):37.17ºN,3.52ºW
- Enete et al. (2012)
- Engelbrecht et al. (2009)
- Engelbrecht et al. (2014):28.07ºN,15.45ºW
- Falkovich et al. (2001):32.08ºN,34.8ºE
- Ferguson et al. (1970)
- Fiol et al. (2005):39.63ºN,2.65ºE
- Formenti et al. (2008):13.5ºN,2.6ºE
- Game (1964):25.07ºN,20.73ºW
- Ganor (1991):31.78ºN,35.22ºE
- Ganor et al. (2000)
- Gaudichet et al. (1989):34.78ºS,77.52ºE
- Gaudichet et al. (1992)
- Glaccum and Prospero (1980)
- Goldberg and Griffin (1970)
- Jeong (2008):37.5ºN,126.92ºE
- Jeong and Achterberg (2014)
- Jeong et al. (2014)
- Johnson (1976)
- Kandler et al. (2007):28.32ºN,16.5ºW
- Kandler et al. (2009):30.24ºN,5.6ºW
- Kandler et al. (2011):14.94ºN,23.48ºW
- Khalaf et al. (1985)
- Leinen et al. (1994)
- Lu et al. (2006):40ºN,116.77ºE
- Menendez et al. (2007):27.97ºN,15.6ºW
- Møberg et al. (1991):11.07ºN,7.7ºE
- O'Hara et al. (2006)
- Parkin et al. (1970)
- Parkin et al. (1972)
- Prospero and Bonatti (1969)
- Prospero et al. (1981)
- Queralt-Mitjans et al. (1993)
- Rashki et al. (2013)
- Shao et al. (2008):39.99ºN,116.34ºE
- Shen et al., (2006):40.5ºN,94.82ºE
- Shen et al. (2009)
- Shi et al. (2005):40ºN,116.77ºE
- Skonieczny et al. (2013):14.41ºN,16.96ºW
- Tomadin et al. (1984)
- Windom (1969)
- Zdanowicz et al. (2006)
- Zhou and Tazaki (1996):35.48ºN,133.07ºE

Mineral Fractions Simple (SMF) vs. New (AMF) Method

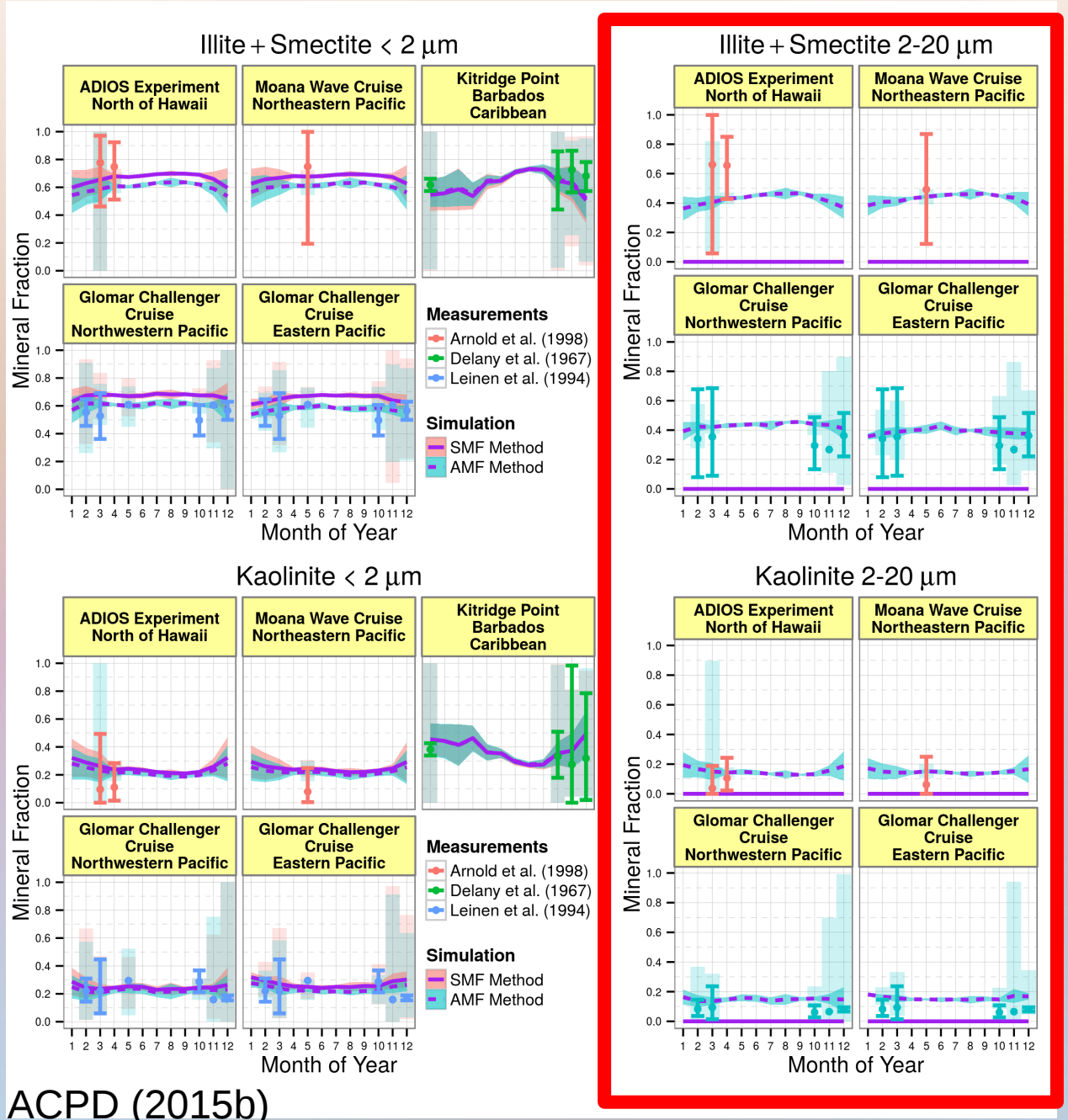

Perlwitz et al., ACPD (2015b)

Mineral Fractions Simple (SMF) vs. New (AMF) Method

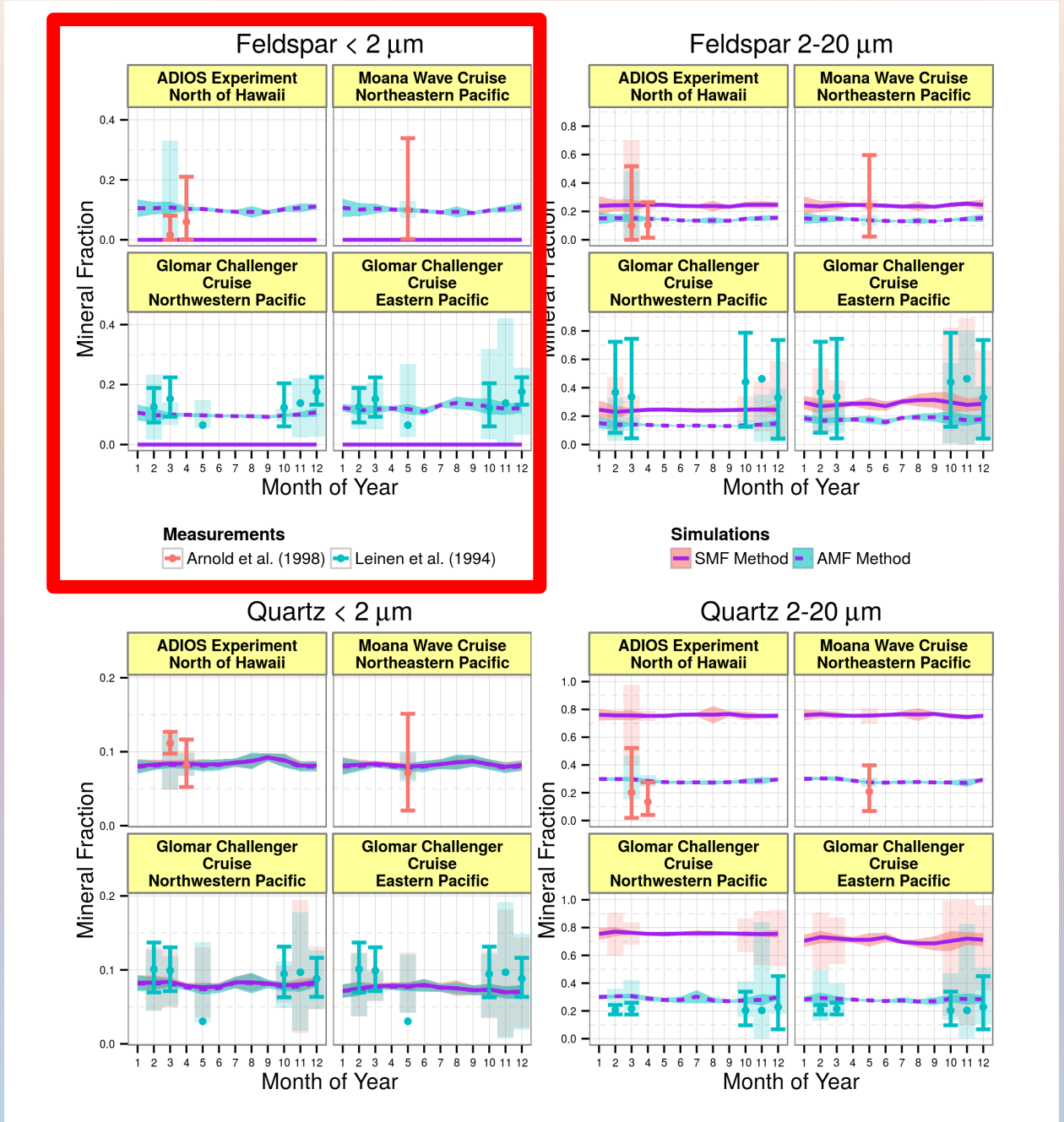

Mineral Fractions Simple (SMF) vs. New (AMF) Method

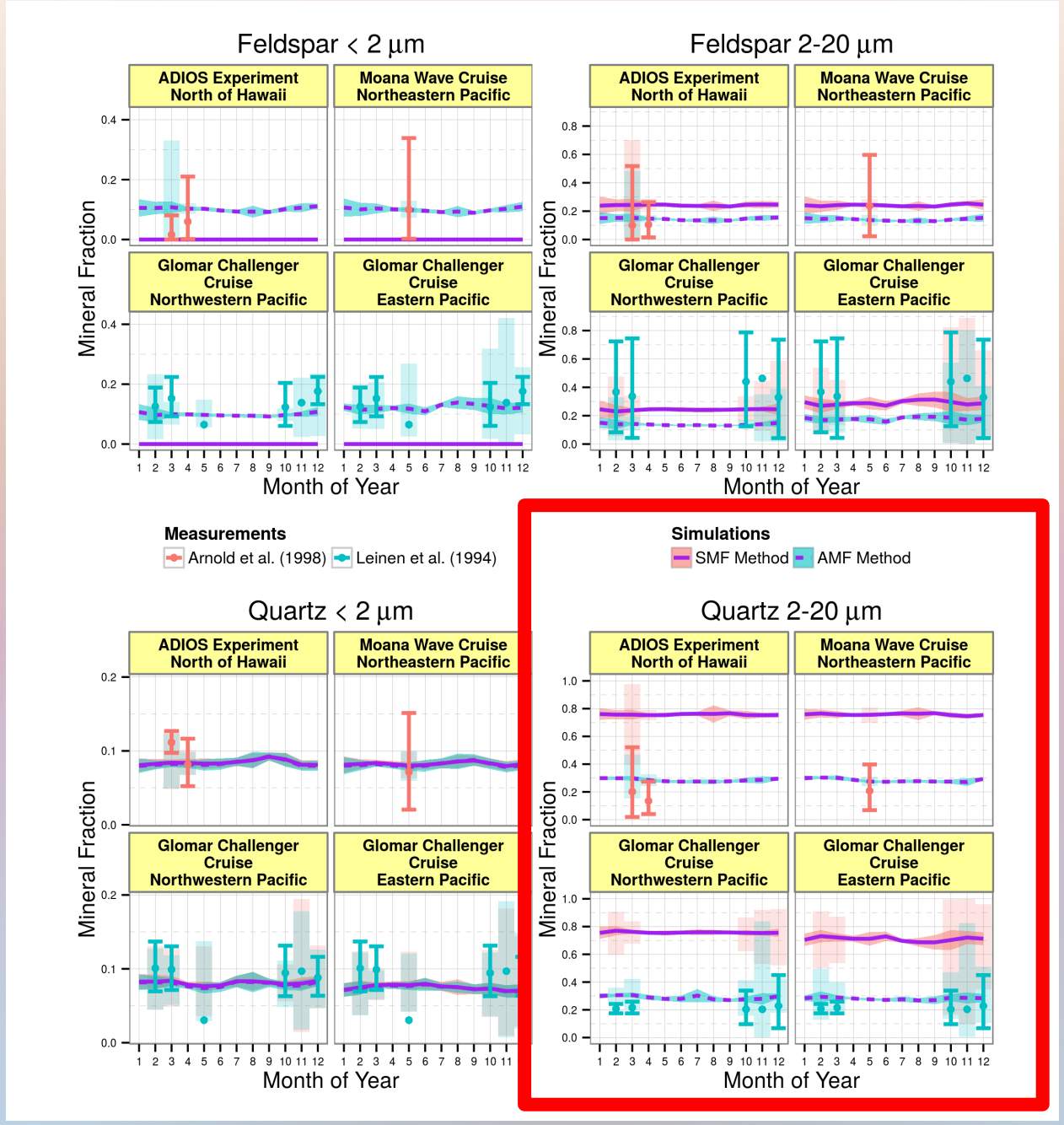

Evaluation - Silt Sized Dust

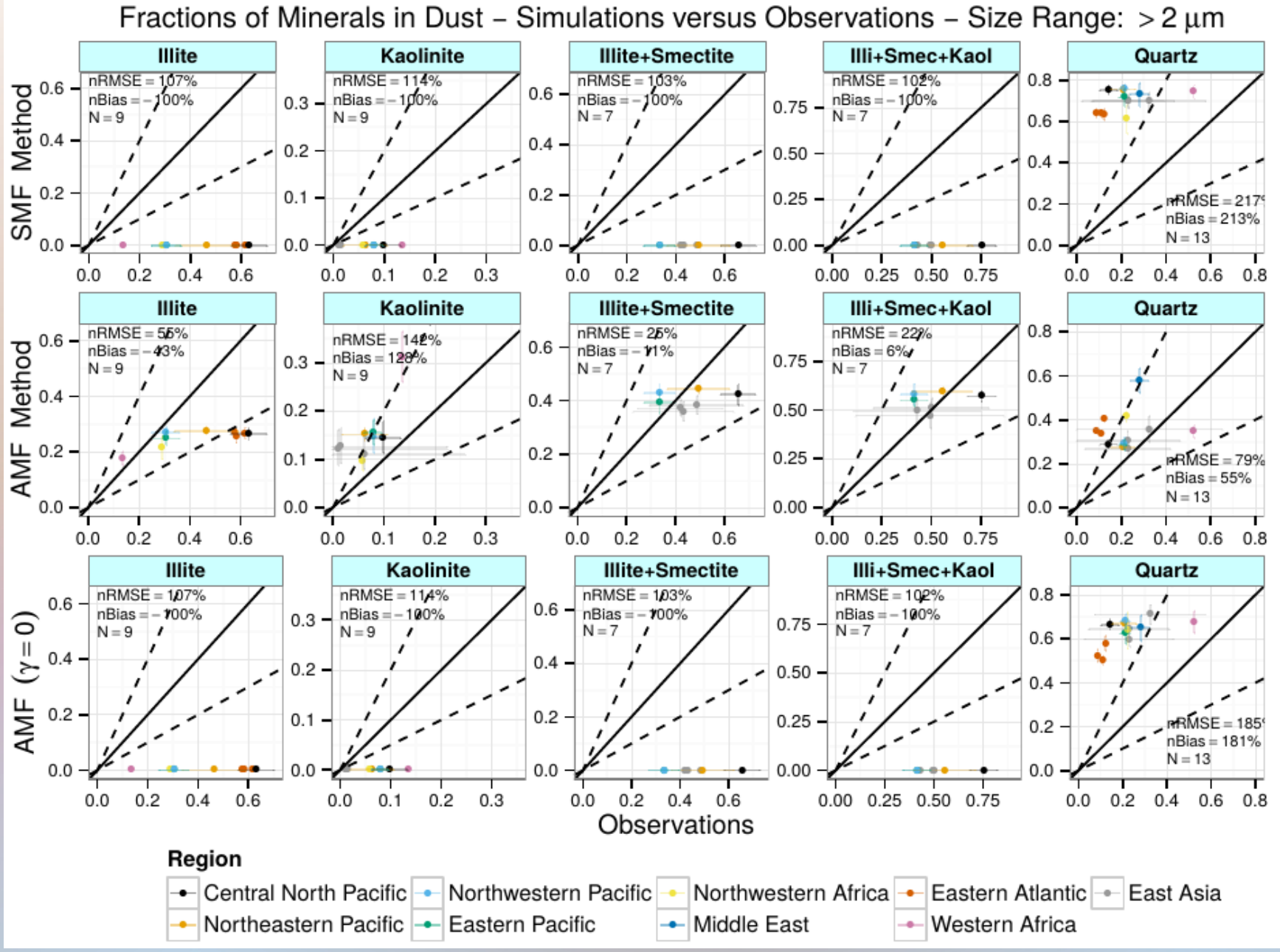

Evaluation - Clay Sized Dust

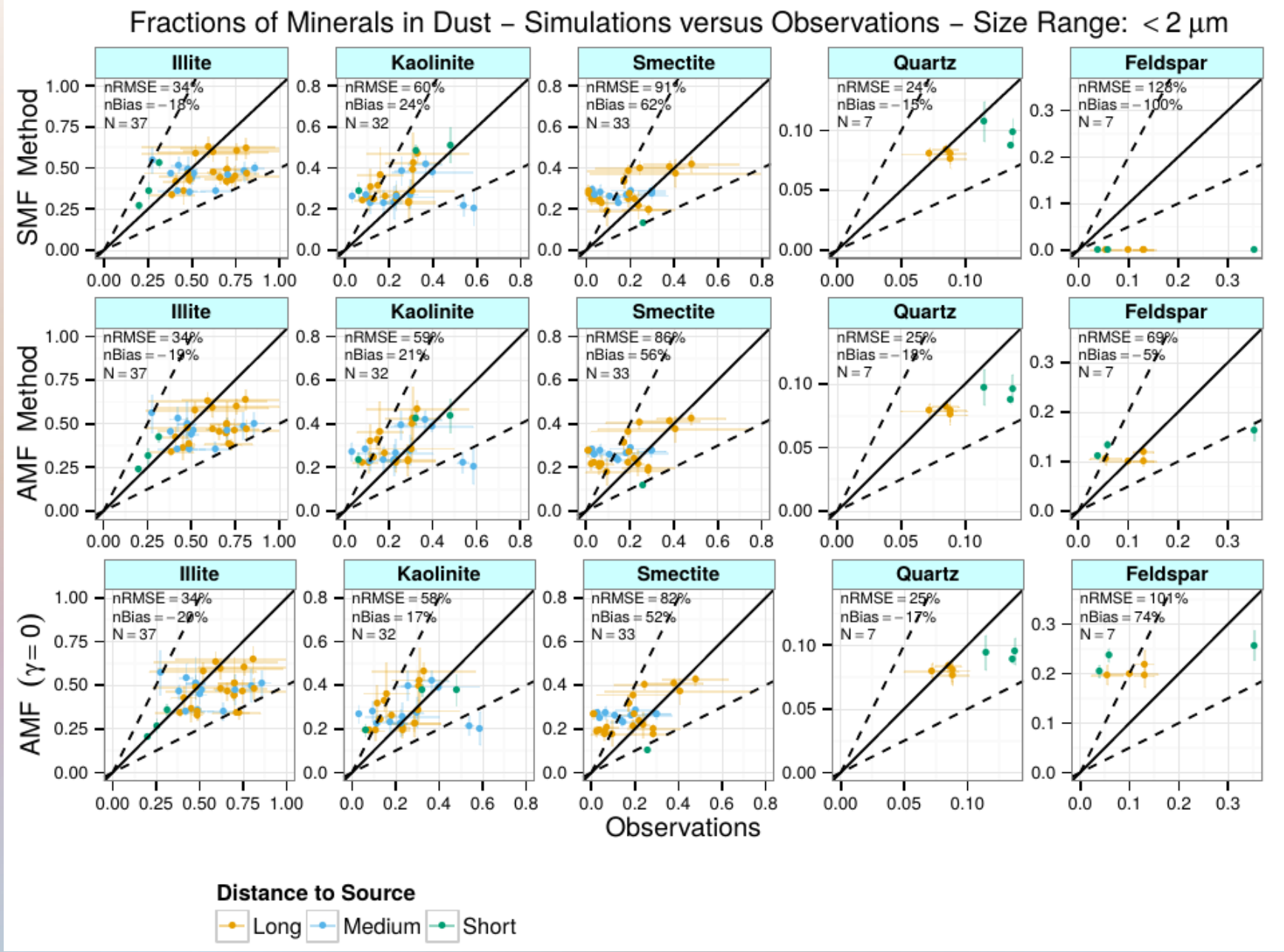

Evaluation - Bulk Dust: Phyllosilicates

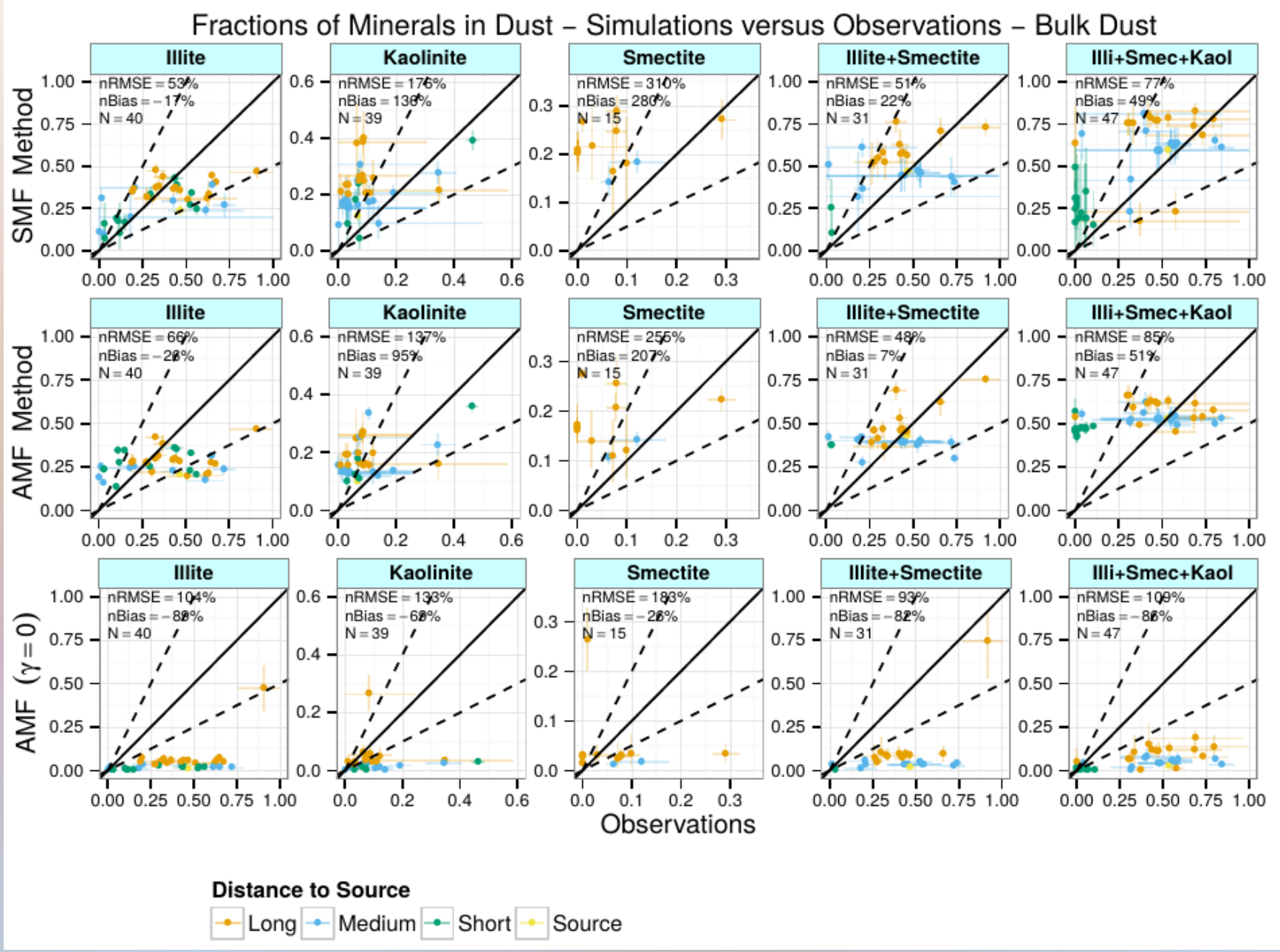

Evaluation - Bulk Dust: Other Minerals

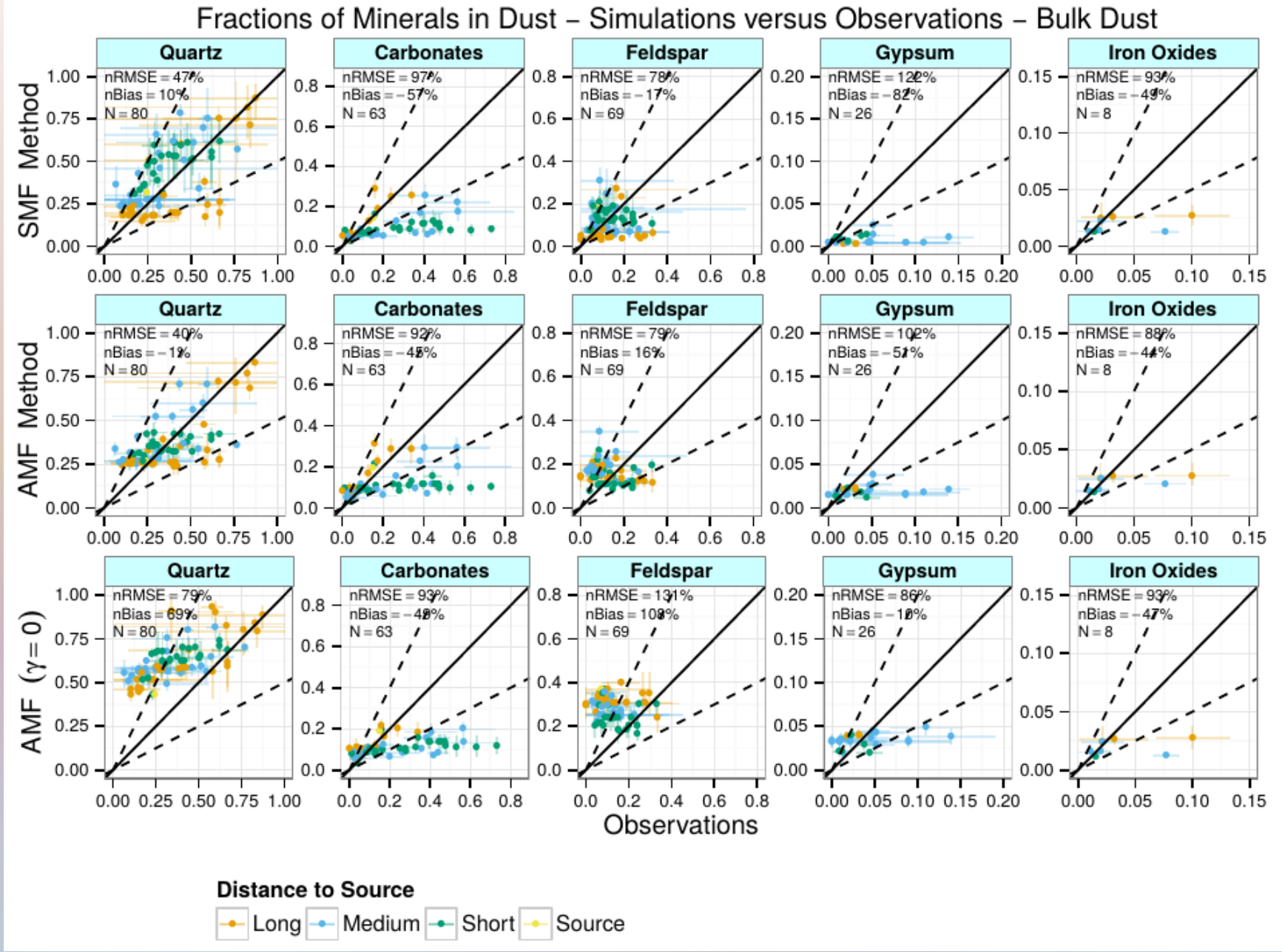

Evaluation – All Sizes Combined

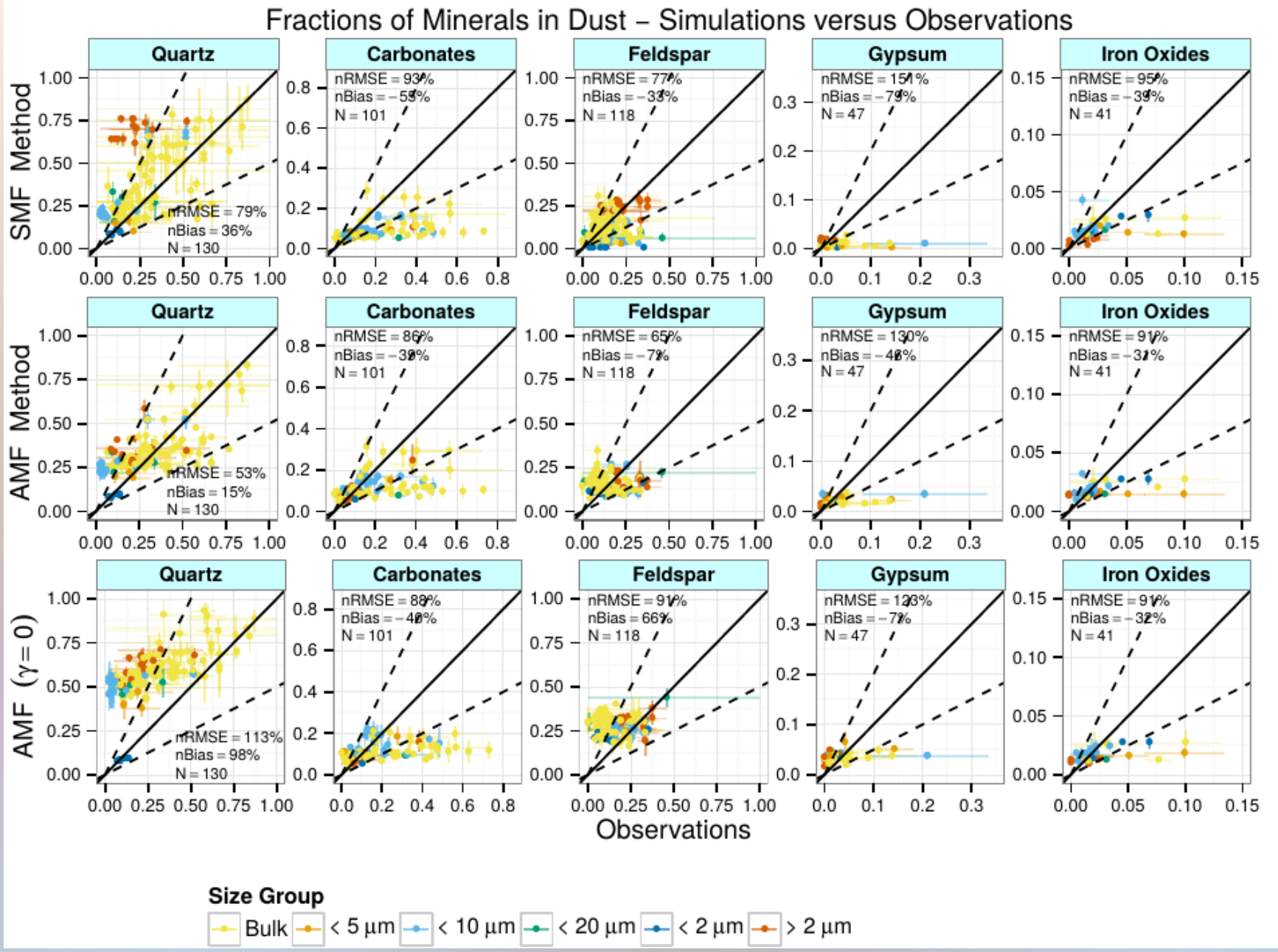

Example for Application: Free and Structural Iron

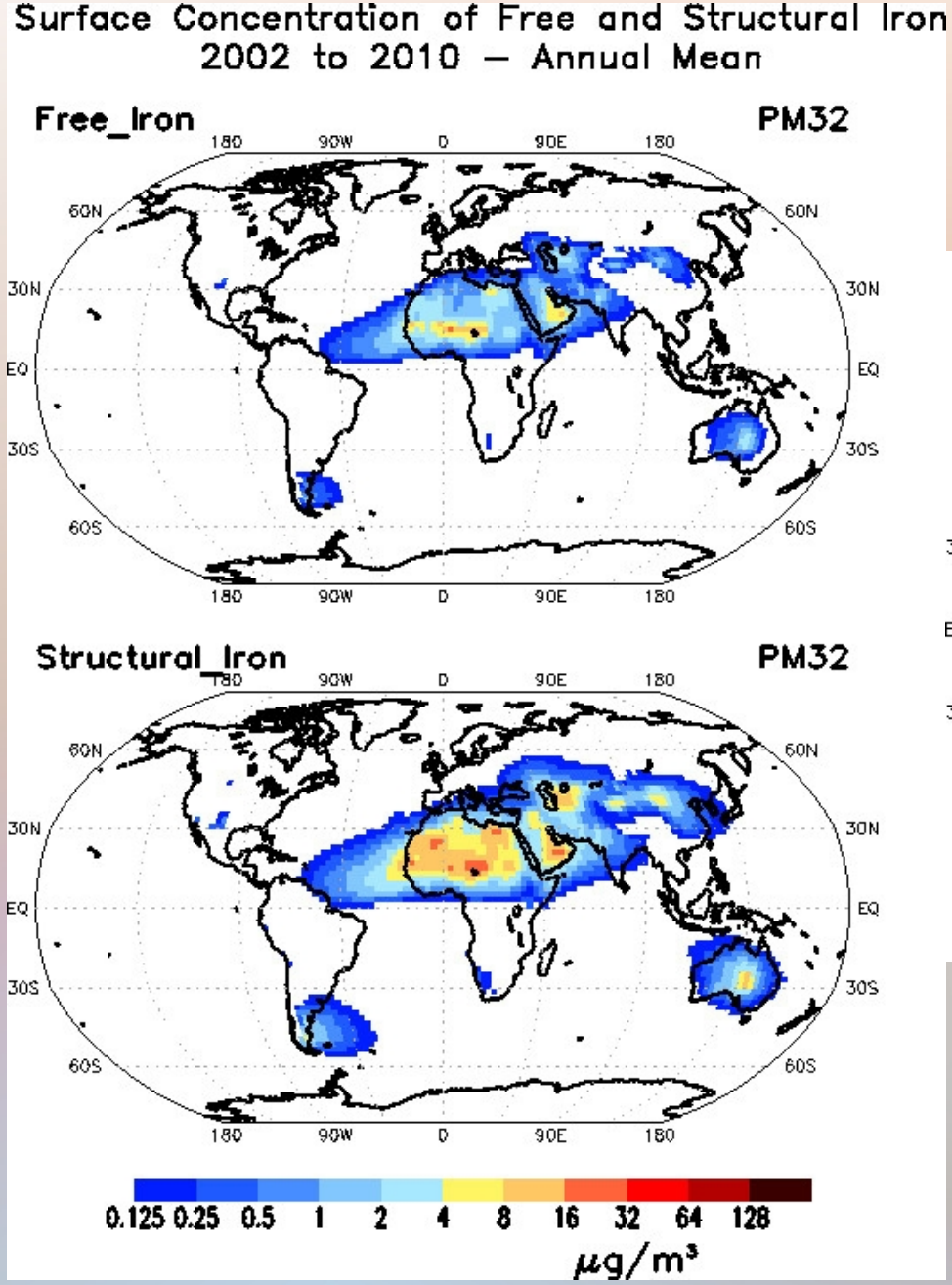

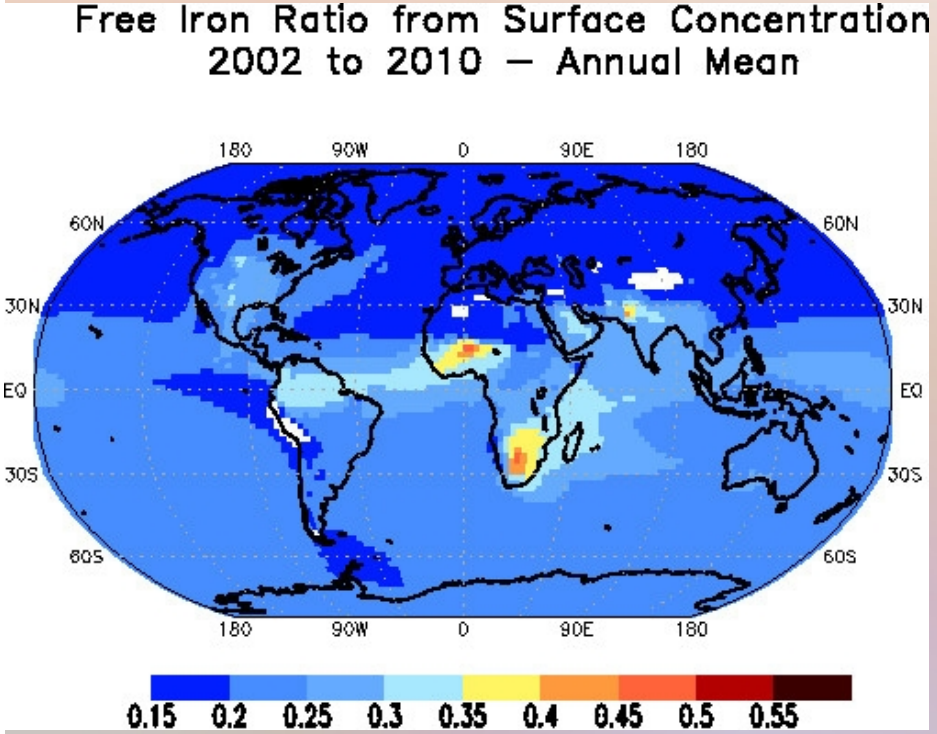

Next Steps: Radiative Effect of Minerals

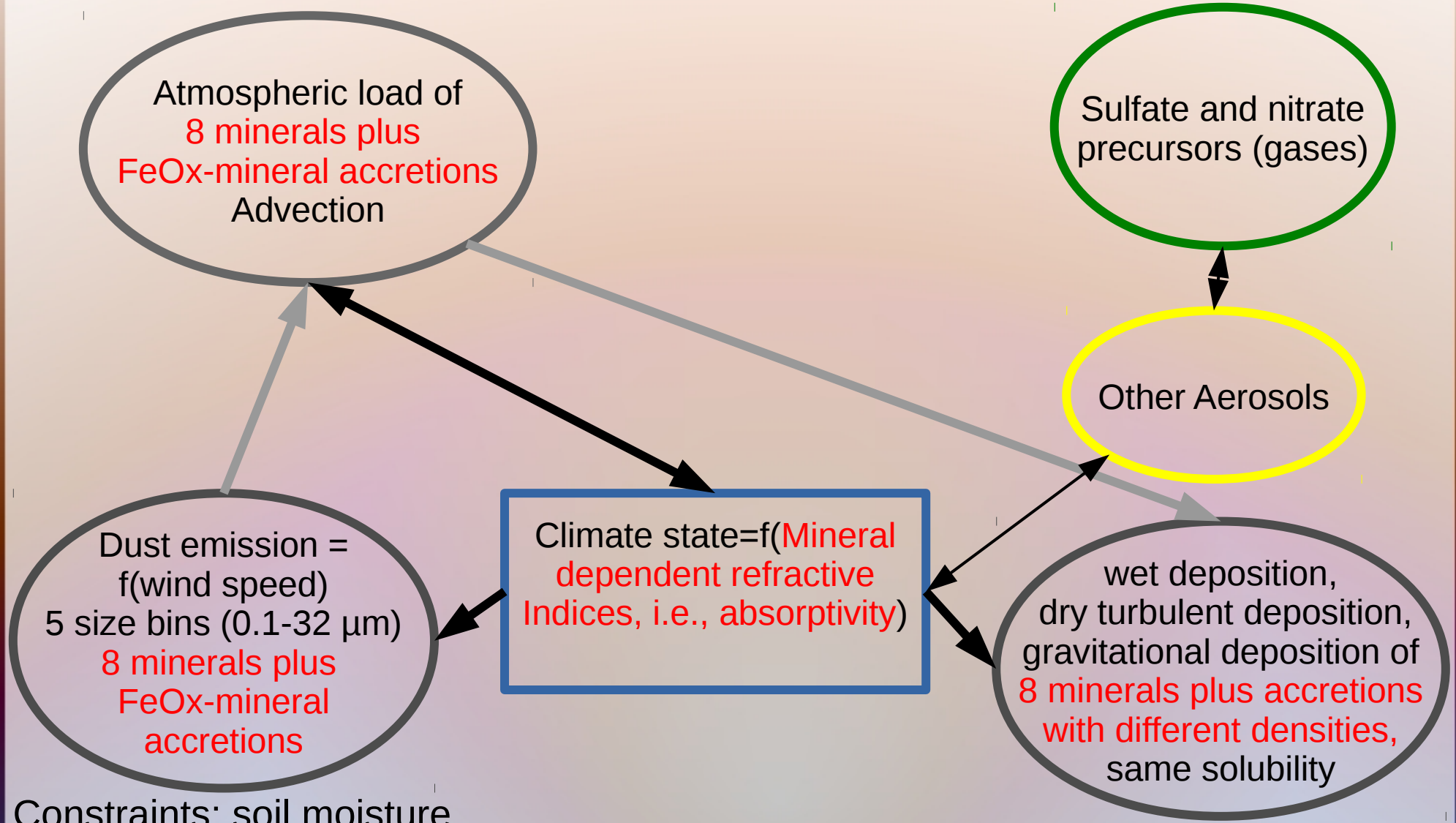

Constraints: soil moisture, vegetation cover, (land use), size dependent mineral composition of soils

Next Steps: Heterogeneous Chemistry of Minerals

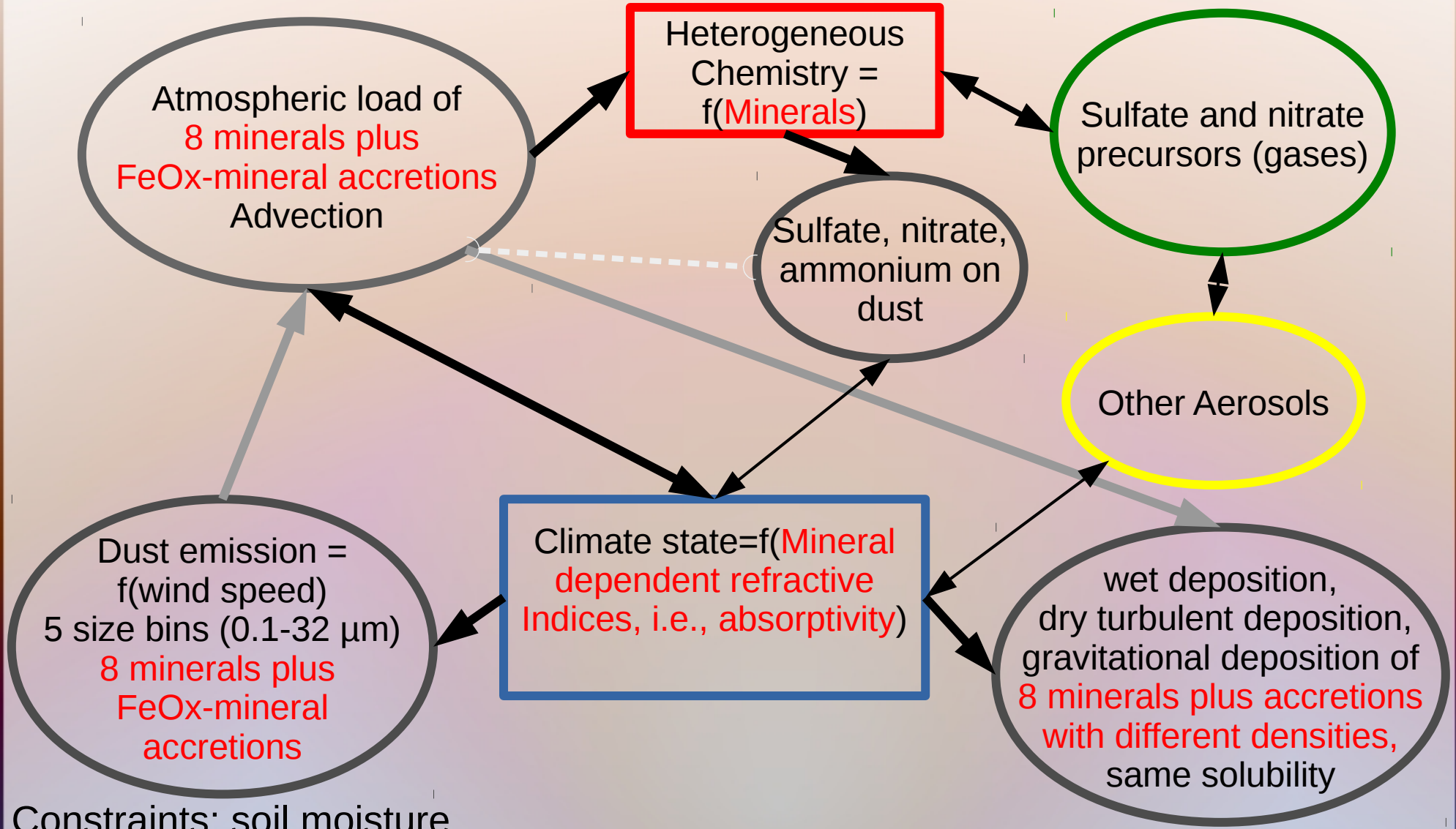

Constraints: soil moisture, vegetation cover, (land use), size dependent mineral composition of soils

Near Future Work: Minerals as CCN and IN (collaborative)

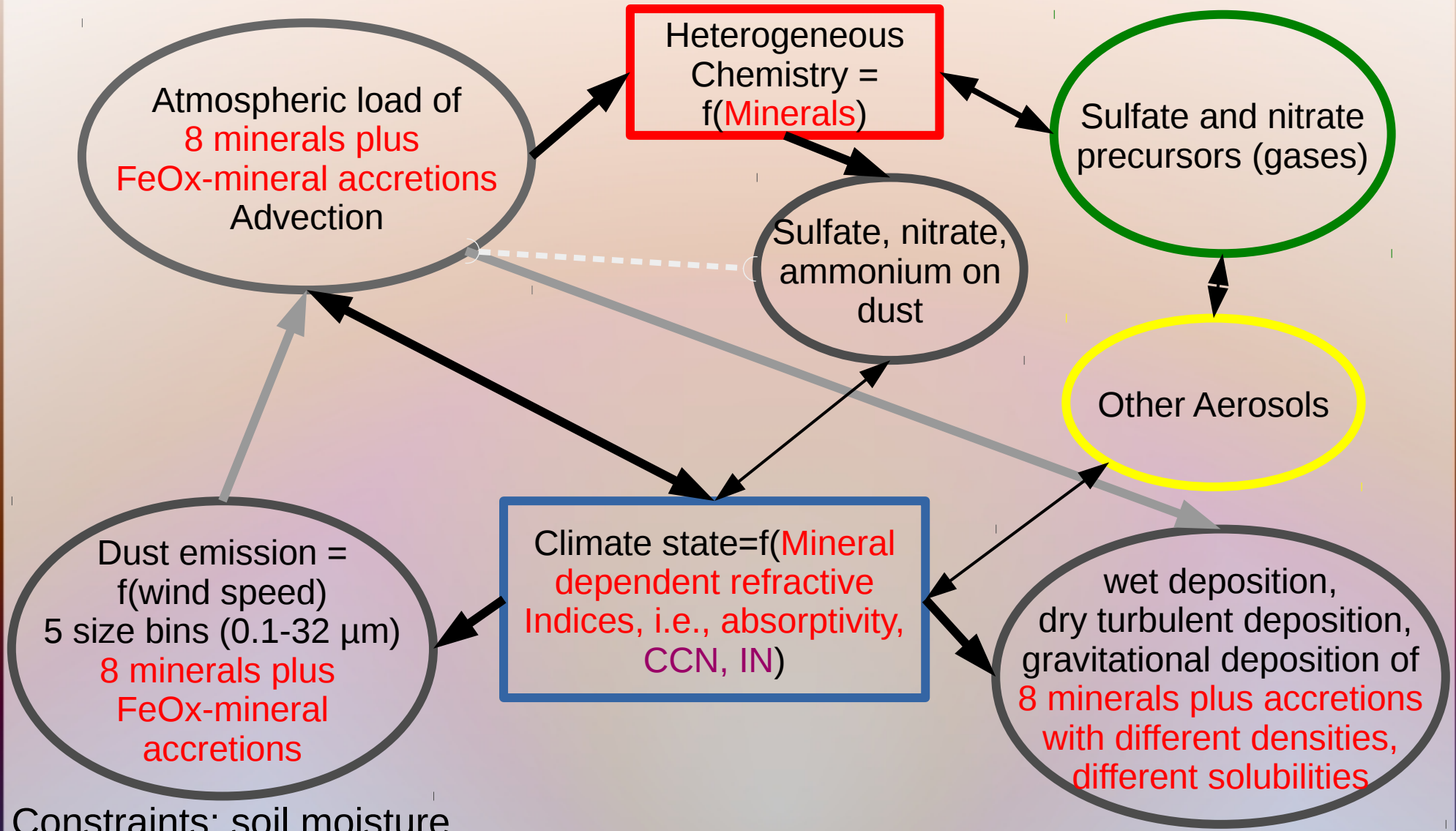

Constraints: soil moisture, vegetation cover, (land use), size dependent mineral composition of soils

Near Future Work: Iron Fertilization (collaborative)

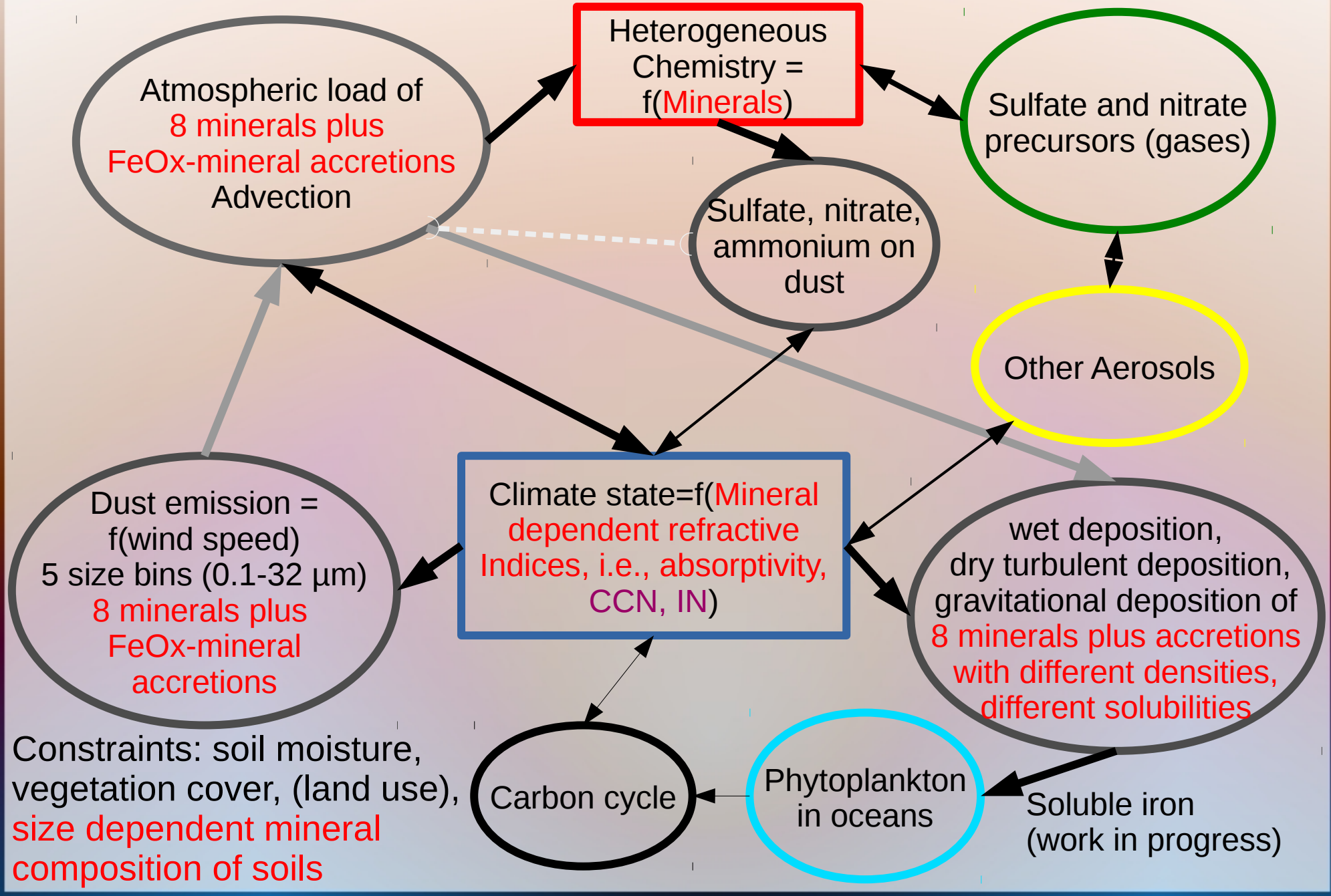

Summary

- We have developed an improved approach for the derivation of the individual mineral species emission from soils, applying Claquin's Mean Mineralogical Table in combination with additional constraints from measurements by using aerosol size distributions for each mineral type
- We simulate emission, transport, and deposition of a mixture of non-accreted minerals and accretions of iron oxides with each of the other minerals in clay and silt size bins
- The agreement between data from measurements and model simulations is encouraging
- Claquin et al./Nickovic et al.' s MMT are very useful data. They have to be properly applied to derive the mineral fractions of dust aerosols

About The Future

In the future, for an improved validation we would need

a) Data from routine measurements of the dust mineralogical composition over longer time periods
b) The elemental composition of minerals, e.g., the amount of structural iron, to be able to use element data for the validation of the simulated mineral cycle
c) More information about aggregation, especially of iron oxides in dust aerosols

Our To Do List (as collaborative efforts)

a) Applying our methodology to the mineralogical table by Journet et al. ACP (2014)
b) Sensitivity studies, variability of mineral composition
c) Simulating iron fertilization (and, in turn, the effect on the carbon cycle), cloud condensation nuclei, ice nuclei, heterogeneous chemistry, radiative forcing of climate as processes dependent on the mineralogical composition of dust
d) Potential for applications for paleo-climate studies

References:

Arnold, E., J. Merrill, M. Leinen, and J. King (1998), The effect of source area and atmospheric transport on mineral aerosol collected over the North Pacific Ocean, Global and Planetary Change, 18(3-4), 137-159, doi:10.1016/S0921-8181(98)00013-7.

Claquin, T., M. Schulz, and Y. J. Balkanski (1999), Modeling the mineralogy of atmospheric dustsources, J. Geophys. Res., 104 (D18), 22,243–22,256, doi:10.1029/1999JD900416.

Kandler, K., L. Schütz, C. Deutscher, M. Ebert, H. Hofmann, S. Jäckel, R. Jaenicke, P. Knippertz, K. Lieke, A. Massling, A. Petzold, A. Schladitz, B. Weinzierl, A. Wiedensohler, S. Zorn, and S. Weinbruch (2009), Size distribution, mass concentration, chemical and mineralogical composition and derived optical parameters of the boundary layer aerosol at Tinfou, Morocco, during SAMUM2006, Tellus, 61B(1), 32–50, doi:10.1111/j.1600-0889.2008.00385.x.

Leinen, M., J. M. Prospero, E. Arnold, and M. Blank (1994), Mineralogy of aeolian dust reaching the North Pacific Ocean 1. Sampling and analysis, J. Geophys. Res., 99, 21,017–21,023, doi:94JD0173510.1029/94JD01735.

Moosmüller, H., J. P. Engelbrecht, M. Skiba, G. Frey, R. K. Chakrabarty, and W. P. Arnott (2012), Single scattering albedo of fine mineral dust aerosols controlled by iron concentration, J. Geophys. Res., 117, D11210, doi:10.1029/2011JD016909.

Nickovic, S., A. Vukovic, M. Vujadinovic, V. Diurdevic, and G. Pejanovic (2012), Atmos. Chem. Phys., 12(2), 845-855, doi: 10.5194/acp-12-845-2012.

Perlwitz, J., and R. L. Miller (2010), Cloud cover increase with increasing aerosol absorptivity: A counterexample to the conventional semidirect aerosol effect, J. Geophys. Res., 115, D08203, doi:10.1029/2009JD012637.

Shao, Y., M. Ishizuka, M. Mikami, and J. F. Leys (2011), Parameterization of size-resolved dust emission and validation with measurements, J. Geophys. Res., 116, D08203, doi:10.1029/2010JD014527.